High-throughput transposon sequencing highlights the cell wall as an important barrier for osmotic stress in methicillin resistant *Staphylococcus aureus* and underlines a tailored response to different osmotic stressors

Short Title: Global analysis of osmotic stress responses in Staphylococcus aureus

Christopher F. Schuster[a], David M. Wiedemann[a], Freja C. M. Kirsebom[a,1], Marina Santiago[b,2], Suzanne Walker[b] and Angelika Gründling[a,3]

ORCID IDs: 0000-0002-4566-7226 (CFS), 0000-0001-6961-0980 (DMW), 0000-0003-4585-319X (FCK), 0000-0002-5446-3452 (MS), 0000-0002-0545-914X (SW), 0000-0002-6235-8687 (AG)

[a]Section of Microbiology and MRC Centre for Molecular Bacteriology and Infection, Imperial College London, London, SW7 2AZ, U.K.

[b]Department of Microbiology and Immunobiology, Harvard Medical School, Boston, MA 02115, U.S.A.

[1]Current address: Section of Respiratory Infections, National Heart and Lung Institute, Imperial College London, London, W2 1PG, U.K.

[3]To whom correspondence should be addressed. Email: a.grundling@imperial.ac.uk

Keywords: osmotic stress, TN-seq, Tradis, NaCl, KCl, Sucrose, *S. aureus*, DUF25380, Pbp2

Abstract

Staphylococcus aureus is an opportunistic pathogen that apart from causing soft tissue infections, is also a frequent cause of foodborne illnesses. One contributing factor for this food association is its high osmotic tolerance allowing this organism to survive commonly used methods of food preservation. How this resistance is mediated is poorly understood, particularly during long-term exposure. In this study, we used TN-seq based screens to identify genes that are involved in the osmotic stress response of *S. aureus* and to determine how responses differ between different osmotic stressors. Although it is generally assumed that a generic osmotic stress response exists, our results revealed distinctly different long-term responses to NaCl, KCl and sucrose stresses. We were able to link numerous previously unknown factors to the osmotic stress response in *S. aureus* and identified the DUF2538 domain containing gene *SAUSA300_0957* (gene *957*) as essential under salt stress. Interestingly, a *957* mutant was less susceptible to oxacillin and showed increased peptidoglycan crosslinking. The salt sensitivity phenotype could be suppressed by mutations in the transglycosylase domain of the penicillin binding protein gene *pbp2*, and these mutations also restored the peptidoglycan crosslinking to WT levels. These results indicate that increased crosslinking of the peptidoglycan can be detrimental and highlight a critical role of the bacterial cell wall for osmotic stress resistance. This study will serve as a starting point for future research on osmotic stress response and help develop better strategies to tackle foodborne staphylococcal infections.

20 **Introduction**

21 *Staphylococcus aureus* is a Gram-positive bacterium that is carried by about 20% of healthy
22 individuals (Wertheim *et al.* 2005). It is also an opportunistic pathogen causing a variety of diseases,
23 including bacteremia, endocarditis, soft tissue infections and food poisoning (Tong *et al.* 2015). One
24 characteristic of *S. aureus* is its ability to grow in the presence of a very high salt concentration of
25 up to 2.5 M, conditions under which other bacteria are unable to survive (Measures 1975), and this
26 has been used extensively for the isolation of staphylococci. This salt tolerance also allows *S. aureus*
27 to thrive in its niches such as the human nares, skin (Wertheim *et al.* 2005) and certain food products
28 (Adams and Moss 2008).

29 In general, the bacterial cytoplasm is hyperosmotic to the environment and can therefore
30 tolerate a certain level of external osmotic stress. However, an increase in the intracellular sodium
31 concentration can lead to mis- and unfolding of proteins and inhibit enzymatic reactions. Hence, *S.*
32 *aureus* must possess strategies to counter the effects of osmotic damage, but these are poorly
33 understood, as most work has been performed in *Escherichia coli* and *Bacillus subtilis*, which possess
34 much lower salt tolerances than Staphylococci.

35 General short term mechanisms of osmotic stress mitigation are the rapid import of potassium
36 into the cell to reduce the influx of sodium and efflux of water (Csonka 1989; Csonka and Hanson
37 1991; Sleator and Hill 2002). However, during prolonged NaCl stress, potassium levels decrease
38 again after its initial accumulation in the cytoplasm of *S. aureus* (Christian and Waltho 1964; Graham
39 and Wilkinson 1992). Subsequently, *S. aureus* accumulates small osmotically active compounds,
40 named compatible solutes (Measures 1975). The most effective compatible solutes in *S. aureus* are
41 glycine betaine and proline (Measures 1975; Anderson and Witter 1982; Miller *et al.* 1991; Bae and
42 Miller 1992; Pourkomailian and Booth 1992; Townsend and Wilkinson 1992), which are imported
43 by specific osmolyte transporters (Bae and Miller 1992; Pourkomailian and Booth 1992). These

44 preferred osmolytes can accumulate in the cell to very high concentrations without negatively
45 affecting cellular processes (Csonka and Hanson 1991). In addition, *S. aureus* can also synthesize
46 compatible solutes *de novo*, as in the case of glutamine (Anderson and Witter 1982), but this process
47 is much slower than the uptake of osmolytes and requires more energy.

48 Consistent with these observations, previous research studying the underlying genetic factors
49 of the *S. aureus* osmotic stress response implicated several osmolyte transporters in this process
50 (Wengender and Miller 1995; Vijaranakul *et al.* 1998; Scybert *et al.* 2003; Schwan *et al.* 2006; Price-
51 Whelan *et al.* 2013). These include the potassium transport systems Kdp and Ktr (Price-Whelan *et*
52 *al.* 2013), the proline transporter PutP (Wengender and Miller 1995; Schwan *et al.* 2006), the arsenic
53 transport system Ars (Scybert *et al.* 2003) and the branched chain amino acid uptake system BrnQ
54 (Vijaranakul *et al.* 1998). In addition, although currently not experimentally verified, it can be
55 assumed that the main glycine betaine uptake system OpuD (Wetzel *et al.* 2011; Zeden *et al.* 2018)
56 is an important factor for osmotic adaptation as glycine betaine uptake reduces sensitivity to NaCl
57 exposure significantly (Miller *et al.* 1991).

58 Despite these multiple countermeasures, exposure of *S. aureus* to osmotic stress such as high
59 salt concentrations also leads to morphological changes, including the formation of larger cells
60 (Vijaranakul *et al.* 1995) and a thickening of the cell wall (Onyango *et al.* 2013). However, if and
61 which genetic factors are required for those processes are currently not well understood. The cell
62 wall of Gram-positive bacteria is an important barrier against osmotic stresses and acts as a
63 counterpart to the pressurized cytoplasm. A major component of the cell wall is peptidoglycan, a
64 polymer consisting of chains of repeating N-acetylglucosamine (GlcNAc) and N-acetylmuramic acid
65 (MurNAc) units that are crosslinked with neighboring chains via short peptides and, in the case of *S.*
66 *aureus,* pentaglycine cross-bridges (Reviewed by (Vollmer *et al.* 2008)). In the past, the contribution
67 of the cell wall towards osmotic stress resistance was often not considered in the bacterial osmotic
68 stress resistance field, presumably because the integrity of the cell wall was assumed to be a

69 prerequisite rather than an active adaptation to survive osmotic stresses. Nevertheless, several
70 possible changes to the cell wall have been observed *in S. aureus* during NaCl stress, such as
71 shortened interpeptide bridges in the peptidoglycan (Vijaranakul *et al.* 1995), an increase in
72 resistance to methicillin (Madiraju *et al.* 1987) and increased autolysis activity (Ochiai 2000;
73 Stapleton *et al.* 2007). In addition to peptidoglycan, other components within the cell envelope,
74 such as teichoic acids and more specifically their modifications with D-alanine (Koprivnjak *et al.*
75 2006) and sugar residues (Kho and Meredith 2018; Mistretta *et al.* 2019) are affected by osmotic
76 stress. Combined, these findings indicate that the integrity of the cell wall is an important
77 requirement for osmotic resistance.

78 Most studies on osmotic stress in *S. aureus* have been conducted using NaCl as the osmotic
79 stressor. The ionic properties of NaCl have important implications on protein stability and activity
80 as its accumulation can lead to denaturation of proteins. A few studies in *S. aureus* have also been
81 performed with non-ionic osmotic stressors such as sucrose, sorbitol glycerol and amino acids
82 (Mitchell and Moyle 1959; Stewart *et al.* 2002; Stewart *et al.* 2005; Schwan *et al.* 2006). All of these
83 different stresses are often used synonymously with osmotic stress, in part influenced by the
84 findings that the initial mitigation of osmotic stress by either salts or sugars can be prevented by the
85 accumulation of potassium and compatible solutes. However, there are potential differences in the
86 long-term adaptation to ionic and non-ionic osmotic stressors, which up to date have not been
87 investigated in detail. It is currently also not known if the adaptations besides the accumulation of
88 potassium and osmolytes are similar or differ depending on the osmotic stressor, and this was
89 addressed as part of this study.

90 Using a transposon insertion sequencing (TN-seq) method (Santiago *et al.* 2015), we
91 determined on a whole genome level genes that are essential or dispensable during long-term
92 osmotic stress caused by exposure to NaCl, KCl and Sucrose. This yielded very different sets of
93 essential and dispensable candidate genes, providing experimental evidence of the distinct nature

94 of these stresses and linking a number of previously unknown factors to the osmotic stress response
95 in *S. aureus*. NaCl stress proved to be the most severe of these three stressors and using further TN-
96 seq screens and experimental verification, several unknown and understudied genes were identified
97 to be essential under salt stress. This included *SAUSA300_0957,* coding for a cytoplasmic protein,
98 which we show here is important for peptidoglycan homeostasis in *S. aureus*. Another protein,
99 which we identified as important during salt stress and essential for peptidoglycan synthesis, is the
100 penicillin binding protein Pbp2, again highlighting a key function of peptidoglycan during NaCl-
101 induced salt stress. Taken together, these experiments highlight the bacterial cell wall as a key player
102 in the salt stress response of *S. aureus*.
103

104 **Results**

105 **Different types of osmotic stresses target different sets of genes**

106 In the literature, osmotic stress is a loosely used term for any accumulation of osmolytes, however
107 the type of ion or osmolyte can potentially have a great impact on how bacteria respond. To address
108 this issue, we determined how the stress responses to different commonly used osmolytes
109 compare. To this end, a highly saturated *S. aureus* transposon library with a promoter-less
110 transposon was prepared using a phage-based delivery system as described in (Santiago *et al.* 2015)
111 and subsequently used for transposon sequencing (TN-seq) experiments (see Supplementary Table
112 1 for details on all TN-seq experiments). The library was propagated for 16 generations in either LB
113 medium with a normal salt concentration of 85 mM NaCl (LBN) or with 0.5 M NaCl, 0.5 M KCl or 1.0
114 M sucrose added (Figure 1A). The molarity of sucrose was doubled to accommodate for the
115 dissociation of the salts into two ions. The culture challenged with 0.5 M NaCl grew the slowest,

116 followed by 1.0 M sucrose, whereas the cells grown in 0.5 M KCl grew similarly to the cells grown in
117 LBN (Figure 1B).
118 As expected, by using a large and good quality transposon library, transposon insertions were found
119 under all conditions in genes throughout the whole genome (Figure 1C). Next, the number of TN-
120 insertions per gene following growth under the NaCl, KCl or sucrose stress condition was compared
121 to the number of TN-insertions per gene after growth in LBN medium (Supplementary Table 2) and
122 in this manner conditionally essential (Supplementary Table S3) and dispensable (Supplementary
123 Table S4) genes identified. Fold-changes in transposon insertions per gene and q-values were
124 plotted in volcano plots (Figure 1D). From this, it was evident that under KCl stress the number of
125 essential and dispensable genes was much lower than for NaCl or sucrose stress, indicating a much
126 less severe effect of KCl on *S. aureus* cells. Sucrose stress also showed a reduced set of essential and
127 dispensable genes compared to NaCl stress, but considerably higher than under the KCl condition.
128 This was also reflected when inspecting the gene lists of the top 30 essential or dispensable genes
129 (Supplementary Table S3 and S4) as in the KCl condition only 15 and 2 genes respectively met the
130 requirements of q-value ≤ 0.05 and a fold-change of 5. To identify common genes between
131 conditions, the fold-change stringency was relaxed to 2-fold and the overlap of genes was visualized
132 in Venn diagrams (Figure 1E, individual genes in Supplementary Table S5). Three genes, namely
133 *SAUSA300_0425* (*USA300HOU_0457*, *mpsA (nuoF)*, a cation transporter of the respiratory chain
134 (Mayer *et al.* 2015)) *SAUSA300*_0750 (*USA300HOU_0796*, *whiA*, a hypothetical protein, possibly
135 involved in cell wall synthesis) and SAUSA300_0846 (USA300HOU_0903, a possible sodium:proton
136 antiporter) were essential in all conditions. In the case of dispensable genes, only one gene,
137 *SAUSA300_1255* (*USA300HOU_1294*, *mprF/fmtC*), coding for a phosphatidylglycerol
138 lysyltransferase involved in the defense against cationic microbial peptides, was identified in all
139 conditions (Figure 1E, Supplementary Table S5). In order to assess similarities and differences on a
140 gene function and cellular pathway level, functional Voronoi maps were generated from the

141 conditionally essential (Figure 2) and dispensable (Supplementary Figure 1) genes regardless of their
142 p-values. These images highlighted the essentiality of the wall teichoic acid through *tagO* and the
143 *dlt* operon (Figure 2A) and the transporters AapA and MgtE in both NaCl (Figure 2A) and KCl (Figure
144 2B) stress conditions. In the high sucrose condition, these transporters were much less prominent
145 (Figure 2C). The patterns of essential genes suggested a similar stress response for the ionic stressors
146 NaCl and KCl that was distinct from sucrose stress. When the dispensable genes were investigated
147 (Supplementary Figure 1), the number and type of genes in the NaCl condition differed considerably
148 from KCl and sucrose stress. Under NaCl stress (Supplementary Figure 1A), in addition to the
149 penicillin binding protein *pbp2*, a large number of genes involved either directly in respiration or
150 indirectly by their role in ubiquinone synthesis were found to be dispensable (Supplementary
151 Figures 1A). The number of dispensable genes in the KCl (Supplementary Figure 1B) and sucrose
152 (Supplementary Figure 1C) conditions were considerably less, indicating differences in the osmotic
153 stress response between NaCl and KCl. Taken together, the overlaps between conditions were small,
154 indicating distinct modes of actions for each osmotic stress.

155 **TN-seq is a robust method to identify *S. aureus* genes involved in NaCl stress**

156 Since the addition of NaCl provided the most stringent selection, we focused our further analysis on
157 the *S. aureus* salt stress response and conducted two additional independent TN-seq screens to
158 confirm the robustness of this approach (Figure 3A). For replicate A, a multiplexed transposon
159 library, generated using 6 different transposons possessing different or no promoters (Santiago *et*
160 *al.* 2015; Coe *et al.* 2019) was used, and for replicate B the same transposon library as described
161 above was used. The libraries were propagated in either LBN or LB medium with 0.5 M NaCl and the
162 expected growth reduction was observed in the presence of 0.5 M NaCl (Figure 3B). The Tn
163 insertions were distributed evenly throughout the genome in the library grown for 17 generations
164 in LBN but became more unbalanced after growth in the high salt medium due to the enrichment

165 of better salt-adapted TN-strains (Supplementary Figure 2). The fold-change of transposon
166 insertions per gene under the salt stress conditions compared to the LBN condition (input library)
167 as well as q-values (false discovery rate according to Benjamini-Hochberg) were determined for each
168 gene (Supplementary Table S6 & S7). The data were again plotted as volcano plots (Figure 3C),
169 revealing similar numbers of conditional salt essential and dispensable genes in both replicates.
170 Furthermore, a good overlap of the top essential and dispensable genes was observed between the
171 replicates confirming the robustness of the TN-Seq screens (Supplementary Tables S8-11).

172 **The TN-seq screens highlight the essentiality of transporters and cell envelope related genes and**
173 **the dispensability of respiration genes under high salt conditions**

174 To provide a visual and genome-wide guide to the cellular functions of conditional salt essential or
175 dispensable genes, Voronoi maps were again generated as described above for the replicate A and
176 B 0.5 M NaCl datasets (Otto *et al.* 2010; Liebermeister *et al.* 2014). In both replicates, genes coding
177 for transporters and cell envelope related genes were the most prominent conditionally salt
178 essential genes (Supplementary Figure S3). More specifically, the TN-Seq data indicated that
179 inactivation of the putative magnesium transporter MgtE (Schuster *et al.* 2019) and the putative D-
180 serine/D-alanine/glycine transporter AapA is detrimental under salt stress. Inactivation of AapA has
181 previously been shown to suppress the temperature sensitivity phenotype seen in an *S. aureus*
182 *fmtC/mprF* mutant (Ishibashi *et al.* 2007) and to lead to increased amoxacillin and daptomycin
183 sensitivity (Mlynek *et al.* 2016; Coe *et al.* 2019). In addition, the *dlt* operon, coding for enzymes
184 required for the D-alanylation of teichoic acids, an important factor for cationic peptide resistance
185 (Brown *et al.* 2013), as well as the stationary and stress sigma factor gene *sigB* were found to be
186 essential.
187 An even larger number of genes was identified as dispensable during salt stress (Supplementary
188 Figure 4). Inactivating or reducing the expression of such genes is expected to help *S. aureus* survive

189 under salt stress. Among these dispensable genes were genes coding for the sodium antiporter
190 Mnh2, which has previously been shown to transport Na^+/H^+ and K^+/H^+ in high pH medium and to
191 play an important role in cytoplasmic pH maintenance (Vaish *et al.* 2018). Strikingly, a large number
192 of genes involved in respiration, such as the *cta/qox/men/hem* operons as well as genes involved
193 indirectly in respiration through quinone synthesis (shikimate pathway, *aro* operon) were also
194 identified as dispensable during salt stress. Curiously, the data also reproducibly indicated that
195 genes coding for the phosphodiesterases GdpP and Pde2 involved in degradation of the signaling
196 molecule c-di-AMP are dispensable under high salt conditions. Somewhat contradictory, the
197 construction of a *dacA* mutant coding for the cognate c-di-AMP cyclase DacA was only possible at
198 high salt concentrations (or in defined chemical medium) (Zeden *et al.* 2018); but altogether these
199 findings confirm the involvement of c-di-AMP in salt mediated osmotic stress adaption in *S. aureus*.

200 **Confirmation of genes essential during salt stress using defined mutants**

201 To determine to what extent different genes identified in the TN-seq screen contribute to the salt
202 resistance of *S. aureus*, a set of candidate genes from the top salt essential genes of dataset B were
203 chosen for further analysis. For this analysis we used defined transposon mutants available from the
204 *S. aureus* NTML transposon mutant library (Fey *et al.* 2013) (Supplementary Table S12). Most of the
205 chosen genes showed similar trends in dataset A, but intriguingly two of the tested genes, *rsbV* and
206 *rsbW*, were flagged as highly dispensable in dataset A but as essential in dataset B. Since no strains
207 with transposon insertions in the *dlt* operon were available in the NTLM transposon mutant library,
208 the contribution of these genes to the salt stress resistance was not further investigated.
209 Next, the growth of the different NTML transposon mutant strains was assessed in LBN and LB 0.5
210 M NaCl medium. In LBN medium, most strains grew similarly to the WT strain JE2, indicating that
211 inactivation of the respective gene does not greatly affect bacterial growth in normal LB medium
212 (Figures 4A-D, left panels). Exceptions were strains NE1109 (*sigB*) (Figure 4A), NE1778 (*lcpB*) (Figure

213 4B) and NE188 (*mfd*) (Figure 4C), cultures of which reached slightly lower final optical densities. At
214 high osmolarity conditions (LB 0.5 M NaCl), all strains showed a growth defect compared to the WT
215 strain (Figures 4A-D), validating TN-seq as a method to identify *S. aureus* genes important during
216 salt stress. Several strains exhibited strong growth defects in the presence of 0.5 M NaCl (Figures 4C
217 and D) with strain NE1384 (*SAUSA300_0957*) showing extremely reduced growth (Figure 4D). To
218 confirm that the salt sensitivity was mediated by the inactivation of the genes in questions, we
219 constructed complementation plasmids for seven of the most promising candidates by either
220 expressing the gene of interest from its native promoter or an anhydrotetracycline (Atet) inducible
221 promoter in the transposon mutant strains. While no complementation was observed for four
222 strains (Supplementary Figures 5A and B), the salt-dependent growth defect could be
223 complemented for strains carrying mutations in *SAUSA300_0694* (Figure 5A), *SAUSA300_0910*
224 (*mgtE*) and *SAUSA300_0957* (Figure 5B). *SAUSA300_0694* encodes a hypothetical protein with 6
225 predicted transmembrane helices but no other identifiable domain motif. MgtE (SAUSA300_0910)
226 is a predicted magnesium transporter. *SAUSA300_0957* (from here on also referred to as gene *957*)
227 codes for a cytoplasmic protein of unknown function and was further investigated in this study
228 because a *957* mutant exhibited the strongest salt-sensitivity phenotype.

229 **Genomic organization of *957* suggests a potential function in cell envelope homeostasis**

230 *SAUSA300_0957* encodes a protein with a DUF2538 domain of unknown function. Proteins with this
231 domain are found mainly in Gram-positive bacteria (Actinobacteria and Firmicutes) (based on an
232 Interpro search, https://www.ebi.ac.uk/interpro/entry/IPR024469). Although a crystal structure of
233 the 957 protein has been deposited in the PDB (3KBY), to our knowledge nothing is known about
234 the actual cellular function of this protein. Transcriptome data (Mäder *et al.* 2016) suggest that gene
235 *957* is in an operon with *lcpB* (Figure 6A). LcpB is one of three wall teichoic acid (WTA) ligases present
236 in *S. aureus* that attaches WTA to the peptidoglycan polymer (Over *et al.* 2011; Chan *et al.* 2013;

237 Schaefer *et al.* 2017). Inactivation of LcpB leads to slightly lower WTA levels in the cell wall, whereas
238 deletion of all three WT ligases completely abolishes WTA anchoring to the cell wall (Chan *et al.*
239 2013). In addition, LcpB cell wall ligase activity was demonstrated *in vitro* (Schaefer *et al.* 2017).
240 *fmtA* is located upstream of the *957* operon and has been proposed to code for an esterase that can
241 remove D-alanine modifications from teichoic acids (Rahman *et al.* 2016) and is involved in
242 methicillin resistance (Berger-Bächi *et al.* 1989). Genes coding for a predicted acetyltransferase and
243 *atl* coding for the major *S. aureus* autolysin are found immediately downstream of the *957* operon
244 (Oshida *et al.* 1995). In this early work, gene *957* was first described as an ORF of "unknown
245 function". Since functionally related genes often cluster together in bacteria, this prompted us to
246 next look at cell-envelope related phenotypes for a *957* deletion strain.

247 **Deletion of gene *957* causes physiological changes leading to a smaller cell size**

248 As all previous experiments were performed with transposon mutants, we first constructed strain
249 LAC*Δ*957* with a marker-less in-frame deletion of gene *957*. Strain LAC*Δ*957* had the expected
250 growth defect in the presence of 0.5 M NaCl, which could be complemented by expressing a
251 functional copy of *957* (Figure 6B). We then proceeded to test if the *957* mutant displays other
252 phenotypes and to investigate if gene *957* is involved in cell envelope homeostasis. First, WT LAC*,
253 the *957* mutant and the complementation strain were grown in LBN and the ratio of colony forming
254 units to optical density (CDU/OD) was determined. The CFU/OD ratio was significantly larger for the
255 *957* mutant (60.8±6.8 x10^7 CFU/OD) mutant as compared to strain LAC* (37.5±9.3 x10^7 CFU/OD)
256 when grown in LBN, suggesting a change in cell shape or size (Figure 6C). This phenotype was
257 restored in the complementation strain (37.3±3.6 x10^7 CFU/OD) (Figure 6C). When the average cell
258 diameter was determined by microscopy, a small but significant reduction in cell diameter was seen
259 for the *957* mutant (1.25±0.02 µm) as compared to the WT (1.36±0.03 µm) and the cell size was
260 restored to wild type levels in the complementation strain (1.35±0.05 nm) (Figure 6D).

261 **Salt sensitivity of *957* is not due to interaction with LcpB but likely due to changes in peptidoglycan**
262 **crosslinking**

263 Since the gene *957* is on the same transcript as *lcpB* coding for a WTA ligase (Figure 6A), the
264 contribution of WTA to salt stress resistance as well as the contribution of *957* to the attachment of
265 WTA to the cell wall was assessed. Initially the growth of a *tagO* (*tarO/llm*) mutant, a strain unable
266 to produce WTA, was tested in LB and LB 0.5 M NaCl medium. When cells were grown in LBN, they
267 grew normally (Supplementary Figure 6A), but under high salt conditions, the *tagO* mutant showed
268 reduced growth, similar to that of the *957* mutant (Figure 7A). This is consistent with what has been
269 reported previously for a *Staphylococcus epidermidis tagO* mutant (Holland *et al.* 2011) and
270 indicates an important role for WTA during salt stress. When the *lcpB* mutant was propagated in
271 LBN medium, its growth was slightly inhibited (Supplementary Figure 6A). However, in high salt
272 medium (Figure 7A) it grew unimpeded and like WT. Since the *lcpB* mutant did not show a growth
273 defect in high salt medium, this made it unlikely that *957* is a regulator of LcpB activity. To further
274 exclude that gene *957* could be somehow involved in the attachment of WTA to the peptidoglycan,
275 we isolated WTA from strains grown in either LB or LB containing 0.4 M NaCl and separated the
276 polymer on native polyacrylamide gels. The slightly lower concentration of salt was chosen because
277 growth of the *957* and the *tagO* mutants was too strongly inhibited at 0.5 M NaCl. As expected the
278 *tagO* mutant did not produce any WTA (Supplementary Figure 6B, Figure 7B) and consistent with
279 previous studies (Over *et al.* 2011; Chan *et al.* 2013), the *lcpB* mutant exhibited slightly reduced WTA
280 levels compared to all other strains (Supplementary Figure 6B, Figure 7B). There was no reduction
281 of WTA observable in the *957* mutant compared to the WT strain in either LBN (Supplementary
282 Figure 6B & 6C) or LB 0.4 M NaCl (Figure 7B & 7C) but rather a small, complementable increase,
283 suggesting no influence of *957* over LcpB on WTA attachment.
284 Gene *957* is found upstream of the bi-functional autolysin gene *atl* and therefore we next
285 investigated potential changes in autolytic activity using zymograms. Cell extracts from overnight

286 cultures of the WT, the *957* mutant and the complementation strain were separated on
287 polyacrylamide gels with embedded *Micrococcus luteus* cells and incubated overnight in buffer to
288 re-fold the autolysins and enable the digestion of the peptidoglycan. A small increase in autolytic
289 activity was detected in the *957* mutant (Figure 7D) for bands around 55 kDa and 70 kDa compared
290 to the WT and complementation strain, indicating a possible change in Atl availability. We also
291 tested the susceptibility of the *957* mutant towards the cell wall active beta-lactam antibiotic
292 oxacillin. In contrast to our expectations, the *957* mutant exhibited a small but significant increase
293 in MIC towards this antibiotic than the WT or the complementation strain (Figure 7E), indicating
294 potential changes to the peptidoglycan structure. To test this, we next analyzed the muropeptide
295 profile of mutanolysin-digested peptidoglycan isolated from the WT, the *957* mutant and
296 complementation strain after growth in LBN or LB 0.4 M NaCl medium. Upon first inspection, no
297 peaks were absent in any condition or strain (Supplementary Figure 6D, Supplementary Figure 6E).
298 Probing further, mono- and multimers of muropeptides up to 7-mers (see Supplementary Figure 6D
299 for how binning was performed) were quantified but no significant changes were found when
300 strains were cultured in LBN medium (Supplementary Figure 6F). However, when the muropeptide
301 profiles from cells cultured in 0.4 M NaCl were compared, a significant decrease in the total amount
302 of di- and trimers and a significant increase in higher multimers was observed for the peptidoglycan
303 isolated from the *957* mutant (Figure 7F), suggesting that sensitivity to NaCl could potentially be
304 caused by higher crosslinking and rigidity of the peptidoglycan in the mutant.

305 **Salt-resistant suppressors possess variations in the transglycosylase domain of Pbp2 and show**
306 **reduced peptidoglycan crosslinking**

307 Next, we attempted to generate *957* suppressor strains that showed improved growth in the
308 presence of 0.5 M NaCl, with the idea that by mapping and investigating the compensatory
309 mutations, further insight into the cellular functions of protein 957 could be gained. We initially

310 attempted to raise suppressor strains on solid medium but failed to do so, because the growth
311 defect of the *957* mutant was not as prevalent on agar plates. We therefore used liquid medium
312 instead, where we readily obtained suppressor strains. These strains grew as well as or even better
313 than the WT LAC* strain in the high salt conditions (Figure 8A) and also grew similar to the WT in
314 LBN (Supplementary Figure 7A). The genome sequences of 10 independent suppressor strains were
315 determined and single nucleotide polymorphisms (SNPs) in one or two genes could be identified for
316 each strain (Supplementary table S13), except for one strain where the coverage was insufficient,
317 and this strain was omitted from further analysis. A common denominator for all suppressor strains
318 were SNPs in the *pbp2* gene, coding for the Penicillin binding protein 2 (Pbp2) (Figure 8B). *S. aureus*
319 Pbp2 is a bifunctional enzyme (Wyke 1984; Murakami *et al.* 1994), which possesses transglycosylase
320 and transpeptidase activity and is involved in peptidoglycan synthesis. All nine discovered SNPs were
321 unique and led to mutations in the amino acid sequence in the transglycosylase domain but neither
322 to stop codons, nor frameshifts nor mutations in the transpeptidase domain. The mutations were
323 mapped (Figure 8B) onto an available Pbp2 structure (3DWK) (Lovering *et al.* 2008) to see if a specific
324 area of the transglycosylase domain had been targeted, but the amino acid substitutions were found
325 throughout the molecule and not only in the active site. Interestingly, *pbp2* also appeared to be
326 considerably less important for growth at 0.5 M NaCl (Supplementary Figure 7B and 7C), although
327 transposons were mainly localized at the beginning and end of the gene or within the promoter
328 region.
329 To confirm that the *pbp2* SNPs were indeed responsible for the suppression of the salt sensitivity of
330 the *957* mutant, we transferred the *pbp2* SNPs from two strains into a fresh LAC*Δ*957* background
331 by co-transduction of a transposon in a nearby gene (Supplementary Figure 7D, schematic). As
332 expected, these "recreated" suppressor strains showed also increased salt resistance (Figure 8C,
333 Supplementary Figure 8A). In addition, we repaired the *pbp2* gene in two suppressors to the WT
334 *pbp2* allele and this reduced their ability to cope with NaCl stress, all consistent with the hypothesis

335 that the SNPs in *pbp2* are responsible for the suppression phenotype (Figure 8D, Supplementary
336 Figure 8B). When the same *pbp2* SNPs were transferred into a WT LAC* strain, a reproducible
337 growth improvement of the SNP-bearing strains was observed in high salt medium, an indication
338 that the *pbp2* mutations lead to a general growth improvement of *S. aureus* under NaCl stress
339 conditions (Figure 8E, Supplementary Figure 8C).

340 Moenomycin is a phosphoglycolipid antibiotic that inhibits the transglycosylase activity of the *S.*
341 *aureus* Pbp2 enzyme (reviewed in (Ostash and Walker 2010)). To test if a decrease in Pbp2
342 transglycosylase activity results in the improved growth of the *957* mutant in high salt conditions,
343 cells were grown on LB agar containing 0.5 M NaCl with or without moenomycin. The growth
344 behaviors of the WT strain and the *957* mutant were similar when grown on solid LB agar containing
345 0.5 M NaCl but lacking moenomycin (Figure 8F, top panel). As stated above, this discrepancy in the
346 growth behavior of the *957* mutant in high salt liquid versus solid medium was already noted when
347 we attempted to generate suppressors on agar plates. On the other hand, in medium supplemented
348 with 0.02 µg/ml moenomycin, we observed better growth of the *957* mutant compared to the WT
349 strain (Figure 8F, lower panel). In addition, the *957* mutant also showed improved growth compared
350 to the two suppressor strains S2 and S4 when moenomycin was added (Figure 8F, lower panel).
351 These findings are consistent with the idea that a partial inhibition of the glycosyltransferase activity
352 of Pbp2 can improve the growth of the *957* mutant in high salt medium.

353 Because the LAC*Δ*957* strain showed increased peptidoglycan crosslinking when compared
354 to a WT strain, we hypothesized that the peptidoglycan of the suppressor strains would be again
355 less crosslinked. To test this, the peptidoglycan from two of the suppressor strains grown in LB 0.4
356 M NaCl was isolated, the muropeptide profiles determined and compared to that of the original *957*
357 mutant (Figure 8G, Supplementary Figure 8D). As before, the muropeptide profiles looked similar
358 (Supplementary Figure 8D) but quantification revealed a significant reduction in crosslinked
359 peptidoglycan fragments and a significantly overrepresentation of monomeric and dimeric

360 fragments in the suppressor strains as compared to the original *957* mutant (Figure 8G). These
361 results indicate that the amount of crosslinking of the peptidoglycan polymer is an important factor
362 in the salt resistance of *S. aureus* and that dysregulation of peptidoglycan crosslinking can lead to
363 destabilizing effects.
364

365 **Discussion**

366 In this work, we performed TN-seq screens with *S. aureus* exposed to different osmotic stresses and
367 could show that each osmotic stressor affects a defined but different set of genes. It is therefore
368 important to use the term osmotic stress carefully, as our results highlight that there is not one
369 general osmotic stress response but rather responses tailored to the individual osmolyte. Using TN-
370 seq, we successfully identified several salt tolerance genes in the USA300 *S. aureus* LAC* strain and
371 further characterized gene *957,* a gene without previously assigned function. Our results indicate
372 that the gene product is involved in cell envelope homeostasis but likely not WTA attachment and
373 we show that its absence leads to increased crosslinking of the peptidoglycan. Suppressors of a *957*
374 mutant acquired mutations in *pbp2* and the increase in peptidoglycan crosslinking was reversed in
375 such stains. This demonstrates that the synthesis of the peptidoglycan layer is a tightly regulated
376 process that plays an essential role during osmotic stress.

377 From our TN-seq data and the use of different osmotic stressors (NaCl, KCl and sucrose), it is evident
378 that although all these compounds exert osmotic stress, the response differs greatly between them
379 (Figure 1, Figure 2 and Supplementary Figure S1). NaCl and KCl conditions share a set of genes that
380 become essential such as the transporters *aapA* and *mgtE* (Figure 2A and B) but differ in the set of
381 dispensable genes (Supplementary Figure S1A and B). It is intriguing that a whole set of respiration
382 related genes become dispensable under NaCl stress but not under KCl stress. This could indicate
383 that respiration should be inhibited or slowed down in high NaCl conditions, possibly by interference
384 with sodium pumps a process less likely to be inhibited by potassium ions. The set of essential genes
385 under sucrose conditions (Figure 2C) was vastly different from that of the NaCl and KCl conditions
386 whereas the set of sucrose dispensable genes (Supplementary Figure S1C) looked similar to the KCl
387 set. This highlights the differences in osmotic stress adaptations and serves as a reminder that the

388 type of stressor remains important. Therefore, although the term osmotic pressure is useful in some
389 contexts, it often needs to be taken with a grain of salt.
390 TN-seq experiments provide a wealth of information about the growth ability of single mutants in a
391 mixed population and can therefore quickly and accurately determine genes that are required under
392 certain growth condition. It is however always a concern that a single TN-seq experiment might not
393 be reproducible due to stochastic extinction of individual mutants or certain growth dynamics. In
394 this study, we performed three independent NaCl TN-seq experiments using two different libraries
395 and slightly different experimental setups. Although there were differences between experiments,
396 overall the data for 0.5 M NaCl LB proved to be rather consistent between different runs (Figure 2A,
397 Supplementary Figures S1-4, Supplementary Tables S3-S4, S8-S11) suggesting that a single
398 experiment would be sufficient in most cases.
399 Because TN-seq relies on the selection of strains adapted to certain growth conditions, competition
400 between mutants and subsequent depletion of the input library it is to be expected that this method
401 is ideal for exploring the long-term effects on growth instead of quick, short-term responses to
402 stresses. To evaluate how our TN-seq results compared to previous results from high-throughput
403 studies of *S. aureus* cells grown in high salt conditions, we determined the overlaps between our
404 two 0.5 M NaCl, 17 generation datasets and a microarray data set acquired from cells grown for ~6
405 generations in 2 M NaCl (Price-Whelan *et al.* 2013). To compare the datasets, the *S. aureus* strain
406 COL locus tags used in the microarray study were first converted to TCH1516 locus tags where
407 possible (Supplementary Table S14) and afterwards compared with the final two 0.5 M NaCl, 17
408 generation TN-seq datasets. The overlap between the downregulated (microarray) and dispensable
409 (TN-seq) genes was minimal in both replicates (1 and 7) and also very small for the upregulated and
410 essential genes (both 14). Three operons were consistently essential or upregulated between all
411 datasets: the *cap5*, *SAUSA300_0771-2*, and the *sda* operon. The *cap5* genes are involved in capsule
412 production (Chan *et al.* 2014) and this type of capsule has been previously reported to be induced

413 by the addition of salt (Pöhlmann-Dietze *et al.* 2000). Genes *SAUSA300_0771-2* are hypothetical
414 membrane proteins and presumably part of a threonine/serine exporter (Interpro database IDs:
415 IPR010619 and IPR024528) and the *sda* genes are annotated as L-serine dehydratase components
416 and a regulator protein. Taken together, the low overlap between the microarray and TN-seq data
417 (Supplementary Table S14) further highlights that in our screen we have identified a number of
418 previously unknown salt tolerance genes.
419 Most mutants of potential NaCl essential genes identified in the TN-seq screen proved to be
420 sensitive to 0.5 M NaCl (Figure 4A-D), confirming the effectiveness of the TN-seq screen. In
421 particular, previously uncharacterized genes such as *SAUSA300_0694*, *mgtE,* and the *957* gene could
422 be identified as essential during NaCl stress and their phenotypes could be complemented (Figure
423 5). In our study, we opted not to experimentally validate any of the dispensable genes, as the
424 verification of a growth advantage is more difficult to prove than a growth defect, but these genes
425 will provide interesting starting points for future research. In addition, it will be interesting to
426 investigate higher concentrations of NaCl to see if the same or different genes are flagged as
427 essential and dispensable.
428 Gene *957* was selected for further characterization as part of this study, because it had previously
429 not been linked to NaCl stress and had not been investigated before. As gene *957* and *lcpB* are co-
430 transcribed we initially assumed that protein 957 is involved in WTA attachment via LcpB but we
431 were unable to demonstrate such a link. Instead the *957* mutant exhibited increased muropeptide
432 crosslinking, which could be suppressed by certain *pbp2* SNPs suggesting involvement in
433 peptidoglycan synthesis. We can only speculate if the SNPs identified in *pbp2* increase or inhibit the
434 activity of Pbp2. However, judging by the number of independent SNPs, it seems more likely that
435 the mutations lead to a decrease rather than an increase in transglycosylase activity. In addition,
436 the results from the moenomycin sensitivity experiments using a sublethal antibiotic concentration
437 (Figure 8F) highlights that partial inactivation of the transglycosylase activity of Pbp2 improves the

438 growth of the *957* strain in high salt conditions. This is consistent with the idea that the obtained
439 *pbp2* SNPs lead to a decrease in transglycosylase activity. The absence of frameshift or non-sense
440 mutations can be explained by the importance of the C-terminal transpeptidase domain of *pbp2*
441 (Pinho *et al.* 2001) and this is reflected in the transposon insertion distributions (Supplementary
442 Figure 7B & C). Intriguingly, the suppressor mutants show reduced growth compared to the *957*
443 mutant on moenomycin plates, presumably due to transglycosylation activity being reduced to
444 levels that are detrimental to the cell. At this point it is also unclear how mutations in the
445 transglycosylase domain alter the muropeptide pattern, since the peptide bonds are made by the
446 transpeptidase, not the transglycosylase domain. We hypothesize that a decrease in the efficiency
447 of the glycosylation activity and slowing down the glycan chain synthesis process will reduce the
448 efficiency of the subsequent transpeptidation process, resulting in decreased peptidoglycan
449 crosslinking in the *pbp2* SNP strains. It is also noteworthy that the *pbp2* gene becomes dispensable
450 under NaCl conditions (Supplementary Figure S1A and S4), an additional indicator that Pbp2 activity
451 needs to be avoided under high salt conditions.
452 Interestingly, the *957* mutant exhibited a slightly higher oxacillin MIC than the WT. This is in contrast
453 to what we expected as MICs are determined in 2% (0.342 M) salt medium and this should lead to
454 a growth disadvantage of the mutant. However, when seen in light of the increase in peptidoglycan
455 crosslinking, this could explain the growth advantage of the *957* mutant in the presence of this beta-
456 lactam antibiotic, as this could counter the inhibition of transpeptidases by oxacillin.
457 Although we were unable to determine the exact molecular mechanism, it is clear from our data
458 that gene *957* is involved in cell wall synthesis either directly or indirectly. More generally, our work
459 suggests that the rigidity of the peptidoglycan cell wall is an important factor to counter osmotic
460 stresses and it is conceivable that the more crosslinked cell wall of the *957* mutant is less elastic and
461 therefore easier to break under strong osmotic stress caused by NaCl exposure (Summarized in
462 Figure 9).

463 In conclusion, we have identified a number of previously uncharacterized factors involved in the
464 osmotic stress response of *S. aureus,* which in particular highlighted the importance of the cell
465 envelope and the data generated will provide a great resource for further studies of the
466 staphylococcal osmotic stress response.

467 **Material and Methods**

468 **Growth of bacteria**

469 *E. coli* and *S. aureus* strains were streaked from frozen stock onto Lysogenic Broth (LB) or Tryptic
470 Soya agar (TSA) plates, respectively. For all *E. coli* and most *S. aureus* experiments, the bacteria were
471 grown in LB medium (LB normal, LBN, 10 g Tryptone, 5 g Yeast extract, 5 g NaCl) pH 7.5 or LB medium
472 with extra 0.5 M NaCl, 0.5 M KCl or 1 M sucrose added. For molecular cloning and some other
473 experiments (as indicated in the text), *S. aureus* strains were grown in TSB medium. Growth curves
474 were done in 125 ml flasks with 20 ml of medium without antibiotics. Cultures were inoculated from
475 overnight cultures to a starting OD_{600} of 0.01 and growth was followed by determining OD_{600}
476 readings every one or two hours.

477 **TN-seq experiments**

478 A previously published highly-saturated *S. aureus* USA300 library with a mix of six different
479 transposons was used (Santiago *et al.* 2015; Coe *et al.* 2019). In addition, a new transposon library
480 with only the blunt transposon, was produced using the same techniques as described in Santiago
481 *et al.* (Santiago *et al.* 2015) containing approximately 1.2 million individual clones.
482 In the first experiment (NaCl, KCl and sucrose stress), a tube of the blunt library was thawed on ice
483 and used to set up a 20 ml pre-culture in LBN/Erm 10 µg/ml with a starting OD_{600} of 0.1. This starter
484 culture was grown for 1 hour and subsequently used to inoculate 25 ml of either LBN or LB 0.5 M

485 NaCl without Erm to a starting OD_{600} of 0.00125. When the cultures reached an OD_{600} of
486 approximately 0.3, the cultures were back-diluted 1:100-fold into 40 ml fresh medium and 10-12 ml
487 harvested by centrifugation when the back-diluted culture reached an OD_{600} of approx. 1.0 (16
488 generations). The bacterial pellets were washed once with their respective growth medium and
489 stored at -20°C for further processing.
490 In the second experiment (NaCl, Replicate A), the multiplexed promoter transposon library was used
491 and Erm 5 µg/ml was added to the pre-culture and subsequent cultures in either LBN or LB
492 containing 0.5 M NaCl. Samples were collected at an OD_{600} of about 1.4 (17 generations).
493 The third experiment (NaCl, replicate B) was set up similar to replicate A, however the blunt library
494 was used in this case and Erm 5 µg/ml was only added to the pre-culture.
495 The library preparation for sequencing was done as described previously (Santiago *et al.* 2015).
496 Briefly, genomic DNA was isolated, cut with *Not*I, biotinylated adapters ligated, the DNA cut again
497 with *Mme*I, and fragments ligated to Illumina adapters and the products PCR amplified,
498 incorporating bar codes and the Illumina adaptor sequences P5 and P7. The samples were
499 sequenced on an Illumina HiSeq machine after spiking with 40% PhiX DNA. The data analysis was
500 done using the Tufts Galaxy Server and custom python scripts as described earlier (Santiago *et al.*
501 2015). To this end, the reads were trimmed up to the barcode and de-multiplexed by strain barcode.
502 Due to the variability in the DNA cleavage by the *Mme*I restriction enzyme, the reads that could not
503 be mapped to a barcode were trimmed by an additional base and the process repeated. Reads were
504 then mapped to the USA300_TCH1516 (CP000730.1) genome and a hop table was generated.
505 Statistical analysis (Mann-Whitney tests and Benjamini-Hochberg) was done using custom python
506 scripts (Santiago *et al.* 2015). Further exploration of the data was done using Excel and custom R
507 scripts.

508 ***S. aureus* cell diameter measurements**

509 For cell diameter measurements, *S. aureus* strains ANG4054, ANG4340, ANG4341 were grown
510 overnight (14-20 hours) at 37°C with 180 rpm shaking in 5 ml LBN in the presence of 100 ng/ml Atet.
511 100 µl of these overnight cultures was transferred to a 1.5 ml reaction tube and 1.5 µl of BODIPY-
512 FL-vancomycin (100 µg/ml in phosphate buffered saline) was added to each tube to stain the cell
513 wall. After a 30 min static incubation step at 37°C, 1.5 µl of the suspension was pipetted onto a slide
514 covered with a 1% agarose pad and analyzed by microscopy using an Axio Imager.A2 microscope
515 with an EC Plan-Neofluar 100x/1.30 Oil M27 objective and images recorded using an AxioCam MR
516 R3. Native CZI files were opened in FIJI (Schindelin *et al.* 2012) and cell diameters of 200 cells were
517 measured using the line and measure tool. Only cells without any visible septa were measured.
518 Experiment was conducted five times with independent biological cultures (n=5, 200 cells each).

519 **CFU/OD correlations**

520 The different *S. aureus* strains were grown as described for the cell diameter measurements. Optical
521 densities of cultures were measured as well as 100 µl of 10^{-6} dilutions (made in their respective
522 growth medium) plated onto TSA plates. The next day, the number of colonies were counted and
523 the ratios of OD_{600} to CFU calculated. The experiment was conducted six time with independent
524 biological samples (n=6).

525 **Zymogram assays**

526 The different *S. aureus* strains were grown over night in TSB. The next day, the bacteria from an
527 OD_{600} equivalent of 20 were pelleted by centrifugation for 3 min at 17000 x *g*. The cells were washed
528 twice with 600 µl PBS and subsequently suspended in 50 µl SDS sample buffer. The suspension was
529 boiled for 20 min with interspersed shaking, centrifuged for 5 min at 17000 x *g* and 20 µl of each

530 sample was loaded onto Zymogram gels, which where were prepared as described previously
531 (Atilano *et al.* 2014). Gels were stained and de-stained using methylene blue and water. The
532 experiment was performed twice, and a representative result is shown.

533 **WTA isolation and analysis**

534 Overnight cultures of *S. aureus* strains ANG4054, ANG4340, ANG4341, ANG1575, ANG4290,
535 ANG4748, ANG4749, ANG4759 were prepared in LBN and used to inoculate 50 ml LBN or LB 0.4 M
536 NaCl to an OD_{600} of 0.01. The cultures were incubated at 37°C with shaking until they reached an
537 OD_{600} of 5 to 6. Where appropriate, 10 µg/ml chloramphenicol and 100 ng/ml Atet was also added
538 to the medium. The bacteria from 20-24 ml culture were harvested by centrifugation for 10 min at
539 7000 x *g*. The bacterial pellets were washed with 50 mM 2-(N-morpholino) ethanesulfonic acid
540 (MES) pH 6.5 buffer and stored at -20°C until further use. Pellets were then processed and WTA
541 separated on a 20% native polyacrylamide gel by electrophoresis on a Biorad Protein XL ii cell as
542 described previously (Covas *et al.* 2016) and WTA visualized by silver staining according to the
543 manufacturer protocol. Experiments were done with three biological replicates (n=3) and a
544 representative result is shown.

545 **Peptidoglycan isolation and analysis**

546 Peptidoglycan was prepared as described previously (Corrigan *et al.* 2011) with the following
547 modifications: 0.5 L (ANG4290, ANG4382, ANG4384) or 1.0 L (ANG5054, ANG4340, ANG4341) of LB
548 0.4 M NaCl medium (all strains) or LBN (ANG5054, ANG4340, ANG4341) medium were inoculated
549 to an OD_{600} of 0.01. For strains carrying derivatives of plasmid piTET, the medium was supplemented
550 with 100 ng/ml Atet starting from the pre-cultures. The cultures were grown at 37°C with shaking
551 at 180 rpm until they reached an OD_{600} of 2-3 and bacteria were subsequently harvested by
552 centrifugation. Chromatography of mutanolysin digested peptidoglycan was performed as

553 described previously using an Agilent 1260 infinity system (Corrigan *et al.* 2011) and muropeptide
554 peaks assigned according to de Jonge *et al.* (de Jonge *et al.* 1992). For the muropeptide
555 quantification, a baseline was drawn, the total peak area determined as well as the peak areas for
556 mono- and the different multimer peaks and calculated as percentage of the total peak area. The
557 peak area quantification was done three times for each HPLC chromatogram and average values
558 were calculated. Experiments were done with three biological replicates (n=3).

559 **Data analysis, software and statistics**

560 Data were processed with a combination of Python 3.6 (https://www.python.org), R 3.3 & 3.5
561 (https://www.r-project.org/), RStudio 1.1 & 1.2 (https://www.rstudio.com/), Prism 7 and 8
562 (https://www.graphpad.com), ChemStation OpenLab C.01.05 (https://www.agilent.com/) and
563 Microsoft Excel 15 and 16 (https://www.office.com/). Voronoi images were drawn using
564 Proteomaps V2 (Otto *et al.* 2010; Liebermeister *et al.* 2014) using custom TMD files. Microscopy
565 images were analyzed using FIJI 1.0 (https://fiji.sc/). Statistical analysis was performed with Prism
566 using appropriate tests as described in the figure legends.

567 **Raising of Δ*957* suppressor strains**

568 Multiple independent overnight cultures of strain LAC*Δ*957* (ANG4290) were prepared in 5 ml LBN.
569 These cultures were back diluted the next day into 20 ml LB 0.5 M NaCl to a starting OD_{600} of 0.05
570 and grown for 8-10 hours at 37°C with shaking until the cultures were slightly turbid. 50 µl of each
571 culture was passed into 5 ml of LBN and grown overnight. The next day, appropriate culture dilutions
572 were plated onto LBN agar plates and incubated overnight at 37°C. For each independent culture,
573 multiple single colonies were picked and used to inoculate individual wells of a 96-well microtiter
574 plates containing 100 µl LBN and the plates were subsequently incubated at 37°C in a 96-well plate
575 incubator with shaking at 650 rpm. The next day, a culture aliquot was stored at -80°C, and the

576 cultures were also diluted 1:50 in LB 0.5 M NaCl medium and 20 µl of these diluted cultures used to
577 inoculate 180 µl of LB 0.5 M NaCl medium. The plates were incubated overnight with shaking at
578 37°C and the next morning the growth of the potential *957* suppressor strains compared to that of
579 the original LAC*Δ*957* deletion strain (ANG4290), which showed low growth and the WT LAC*
580 (ANG1575) strain, which showed good growth. For each lineage, four suppressors that showed good
581 growth were streaked out from the previously frozen stocks and subsequently single colonies
582 selected to set up overnight cultures. The deletion of gene *SAUSA300_0957* was confirmed by PCR
583 and after performing growth curves in culture flasks, one strain that showed significant growth
584 improvement compared to the original LAC*Δ*957* (ANG4290) strain was selected from each lineage.
585 These strains were streaked out again for single colonies and used to inoculate an overnight culture,
586 giving rise to the independently raised suppressor strains ANG4381 through ANG4394. The
587 compensatory mutations for several of these suppressor strains were subsequently determined by
588 whole genome sequencing.

589 **Transfer of *pbp2* SNPs by phage transduction**

590 In order to demonstrate that the SNPs in *pbp2* are responsible for the growth rescue of strain
591 LAC*Δ*957* (ANG4290), we transferred two different *pbp2* SNPs by phage transduction into the
592 original LAC*Δ*957* strain as well as repaired these SNPs in the suppressor strains. This was done by
593 placing an Erm-marked transposon in proximity of the *pbp*2 gene allowing at a certain frequency for
594 the co-transduction of the Erm marker and the *pbp2* SNP. To this end, the NTML transposon mutant
595 library strain NE789 (Fey *et al.* 2013) was used, which harbors a transposon insertion in
596 *SAUSA300_1332* (putative exonuclease) about 10 kbp upstream of the *pbp2* gene. *SAUSA300_1332*
597 is expected to be unrelated to salt stress and the cell wall synthesis machinery but close enough to
598 lead to an intermediate rate of co-transference with the *pbp2* SNPs. The transposon from NE789
599 was transduced into WT LAC* (Boles *et al.* 2010) and strain LAC*Δ*957* (ANG4290) using phage Φ85

600 yielding strains ANG4561 and ANG452, respectively. The transposon was also transduced into the
601 suppressor strains ANG4382 and ANG4384 transferring either *SAUSA300_1332::Tn* only, yielding
602 strains ANG4527 and 4528 or transferring *SAUSA300_1332::Tn* as well as replacing the *pbp2* SNP
603 with a WT *pbp2* allele yielding *pbp2* repaired strains ANG4557 and ANG4568. Lysates from strains
604 ANG4527 and 4528 (suppressors containing *pbp2* SNPs and *SAUSA300_1332::Tn*) were used to
605 transfer the *pbp2* SNPs back into a clean LAC*Δ*957* strain background yielding strains ANG4624 and
606 ANG4625 and into WT LAC*, yielding strains ANG4563 and ANG4564. Successful repair or transfer
607 of the SNPs was checked by PCR and subsequent restriction digest of the product choosing enzymes
608 that recognize sites present in either the WT or SNP allele (ANG4382 *pbp2* SNP: BsrI. Recognition
609 site CCWGG, additional site introduced by SNP; ANG4384 *pbp2* SNP: SspI. Recognition site: AATATT,
610 site missing in SNP).

611 **Determination of oxacillin MICs using Etest strips**

612 *S. aureus* strains LAC* piTET (ANG4054), LAC*Δ*957* piTET (ANG4340) and the complementation
613 strain LAC*Δ*957* piTET-*957* (ANG4341) were grown overnight (22 hours) in 5 ml TSB containing 10
614 µg/ml chloramphenicol and 100 ng/ml Atet. The next day, the cultures were diluted to an OD_{600} of
615 0.1 in sterile PBS buffer and streaked with cotton swabs onto cation adjusted Mueller-Hinton agar
616 plates supplemented with 2% NaCl and 100 ng/ml Atet. One M.I.C.Evaluator strip was placed on
617 each plate and the plates were incubated for 24 hours at 35°C. MICs were then read directly from
618 the strips. The experiment was done with 4 biological replicates (n=4).

619 **Moenomycin growth improvement test**

620 *S. aureus* strains LAC* (ANG1575), LAC* Δ*957* (ANG4290), LAC* Δ*957* S2 (ANG4382) and LAC* Δ*957*
621 S4 (ANG4384) were grown overnight (18 hours) in 5 ml LBN. The next day, the cells were diluted to
622 an OD_{600} of 0.01 in LBN, grown until mid-exponential phase (OD_{600} 0.4-0.6) and normalized to an

623 OD_{600} of 0.1. The cells were 10-fold serially diluted and 5 µl of each dilution spotted onto LB agar
624 containing 0.5 M NaCl with either 0.02 µg/ml moenomycin (mix of moenomycin A, A12, C1, C3 and
625 C4, Santa Cruz Biotechnology) or no moenomycin. Plates were incubated at 37°C overnight (18-22
626 hours) and photographed. The experiment was done with 3 biological replicates (n=3) and one
627 representative result is shown.

628 **Whole genome sequencing**

629 Genomic DNA was either isolated using the Promega Gene Wizard kit according to the manufacturer
630 instructions or using chloroform-isoamylalcohol as described previously (Schuster and Bertram
631 2014). DNA was sent off for whole genome sequencing to MicrobesNG, Birmingham, U.K. or libraries
632 prepared using the Illumina Nextera DNA kit and sequenced at the London Institute of Medical
633 Sciences. Short reads were trimmed in CLC workbench genomics (Qiagen), then mapped to a custom
634 *S. aureus* USA300 LAC* reference genome generated in a previous study (Bowman *et al.* 2016) and
635 single nucleotide polymorphisms called based on at least 80% frequency of occurrence. This list was
636 compared to a manually curated list of well non false-positives and these entries were removed.

637 **Nebraska Transposon Mutant Library (NTML) strains and complementation strains**

638 All Nebraska transposon mutant library (NTML) strains and primers used in this study are listed in
639 Supplementary Tables S12, S15 and S16. Transposon insertions in the respective genes were
640 confirmed by PCRs. For complementation analysis, NTML strains NE535 (JE2 *SAUSA300_0867*::*Tn*),
641 NE867 (JE2 *SAUSA300_0483*::*Tn*) were transformed as controls with the empty plasmid pCL55 (Lee
642 *et al.* 1991), yielding strains ANG4326 and ANG4328 and strains NE188 (JE2 *SAUSA300_0481*::*Tn*),
643 NE251 (JE2 SAUSA300_0482::*Tn*), NE526 (JE2 *SAUSA300_0694*::*Tn*), NE736 (JE2
644 *SAUSA300_0910*::*Tn*), NE1384 (JE2 *SAUSA300_0957*::*Tn*) with plasmid piTET (Gründling and
645 Schneewind 2007), yielding ANG4308, ANG4310, ANG4377, ANG4336, ANG4338. The WT strain JE2

646 (Fey *et al.* 2013) was also transformed with both plasmids yielding JE2 pCL55 (ANG4325) and JE2
647 piTET (ANG4307).
648 The complementation plasmid piTET-*481* for strain NE188 (JE2 *SAUSA300_0481::Tn*) was
649 constructed by amplifying the *SAUSA300_0481* gene using primers P2378/P2379, digesting the
650 product with AvrII/BglII and ligating the fragment with plasmid piTET cut with the same enzymes.
651 The plasmid was then introduced into *E. coli* strain XL1-Blue, yielding ANG4139. After shuttling the
652 plasmid through *E. coli* strain IM08B (Monk *et al.* 2012), creating strain ANG4150, the plasmid was
653 integrated into the *geh* locus of NE188 (JE2 *SAUSA300_0481*::*Tn*) yielding strain ANG4309. The
654 complementation plasmid piTET-*482* for strain NE251 (JE2 SAUSA300_0482::*Tn*), piTET-*694* for
655 strain NE526 (JE2 *SAUSA300_0694*::*Tn*), piTET-*910* for strain NE736 (JE2 *SAUSA300_0910*::*Tn*), and
656 piTET-*957* for strain NE1384 (JE2 *SAUSA300_0957*::*Tn*) were constructed in a similar manner using
657 primer pairs P2380/P2381 (*SAUSA300_0482*), P2388/P2389 (*SAUSA300_0694*), P2384/P2385
658 (*SAUSA300_0910*) and P2386/P2387 (*SAUSA300_0957*), respectively. The complementation
659 plasmids were recovered in *E. coli* XL1-Blue yielding strains ANG4140 (SAUSA300_0482), ANG4142
660 (*SAUSA300_0694*), ANG4144 (*SAUSA300_0910*) and ANG4145 (*SAUSA300_0957*), shuttled through
661 *E. coli* IM08B giving strains ANG4151 (*SAUSA300_0482*), ANG4153 (*SAUSA300_0694*), ANG4155
662 (*SAUSA300_0910*) and ANG4156 (*SAUSA300_0957*) and finally introduced in the respective NTML
663 strain yielding the complementation strains ANG4311 (*SAUSA300_0482*), ANG4378
664 (*SAUSA300_0694*), ANG4337 (*SAUSA300_0910*) and ANG4339 (*SAUSA300_0957*).
665 Complementation plasmid pCL55-*483* for strain NE867 (JE2 *SAUSA300_0483*::*Tn*) was made by
666 fusing PCR products of the operon promoter (in front of *SAUSA300_0481*) amplified with primers
667 P2588/P2553 and the *SAUSA300_0483* gene, amplified with primers P2554/P2589 together using
668 primers P2588/P2589. The resulting fragment was cloned into pCL55 using EcoRI/BamHI restriction
669 sites. The plasmid was recovered in XL1-Blue, creating strain ANG4291, shuttled through *E. coli*
670 IM08B (ANG4292) and subsequently introduced into NE867 (JE2 *SAUSA300_0483*::*Tn*) to create

671 strain ANG4327. The complementation plasmid pCL55-*867* for strain NE535 (JE2
672 *SAUSA300_0867*::*Tn*) was constructed in a similar manner, using primers P2590/P2556 and
673 P2557/P2591 to amplify the promoter and *SAUSA300_0867* gene, which were subsequently fused
674 in a second PCR using primers P2590/P2591. The resulting fragment was cloning into pCL55 using
675 EcoRI/BamHI restriction sites and the resulting plasmid recovered in *E. coli* XL1-Blue (ANG4293),
676 shuttling through IM08B (ANG4294) and finally introduced into NE535 (JE2 *SAUSA300_0867*::*Tn*),
677 creating the complementation strain ANG4329.

678 **Construction of *S. aureus* gene deletion and complementation strains**

679 *S. aureus* strains with in-frame gene deletions were constructed by allelic exchange using plasmids
680 pIMAY (Monk *et al.* 2012) and pIMAY* (Schuster *et al.* 2019). The gene deletion plasmids were
681 designed to contain approximately 1000 bp up- and downstream regions around the deletion site,
682 amplified from LAC* genomic DNA (Boles *et al.* 2010), and the first and last 30 bp of the open reading
683 frame to be deleted.
684 For construction of plasmid pIMAY-Δ*957*, the up- and downstream regions of *SAUSA300_0957* were
685 amplified using primers P2370/P2371 and P2372/P2373, spliced together in a second PCR using
686 primers P2370/P2373 and cloned into pIMAY using XmaI/EcoRI. Plasmid pIMAY-Δ957 was recovered
687 in *E. coli* XL1-Blue, creating strain ANG4147, shuttled through *E. coli* IM08B (ANG4159) and
688 subsequently introduced into S*. aureus* LAC*Δ*957*. The allelic exchange to delete *SAUSA300_0957*
689 and to create strain LAC*Δ*957* (ANG4290) was performed as previously described (Monk *et al.*
690 2012). For complementation analysis, the above described plasmid piTET-*957* was integrated into
691 the chromosome of strain LAC*Δ*957*, giving rise to the complementation strain LAC*Δ*957* piTET-
692 *957* (ANG4341). As control, the empty plasmid piTET from ANG4163 was also integrated into the
693 chromosome of LAC*Δ*957* yielding strain LAC*Δ*957* piTET (ANG4340). The *lcpB* (SAUSA300_0958)
694 gene was deleted in a similar manner using primers P2844/P2845 and P2846/P2847 for the first and

695 primers P2844/P2847 for the second PCR and cloning the fragment XmaI/EcoRI into pIMAY. Plasmid
696 pIMAY-Δ*lcpB* was recovered in *E. coli* XL1blue (ANG4740), shuttled through *E. coli* IM08B (ANG4742)
697 and introduced into the *S. aureus* LAC* (ANG4744) and finally yielding the *lcpB* deletion strain
698 LAC*Δ*lcpB* (ANG4748).
699 Plasmid pIMAY*-Δ*957-958* was constructed for the production of an *SAUSA300_0957-0958* (*lcpB*)
700 double mutant strain in which the first 30 bases of *SAUSA300_0957* are fused to the last 30 bp of
701 *SAUSA300_0958* (*lcpB*). This was done using primers P2844/P2848 and P2849/P2373 in the first and
702 primers P2844/P2373 in a second PCR. The fragment was cloned using XmaI/EcoRI into pIMAY*
703 (Schuster *et al.* 2019) and the resulting plasmid pIMAY*-Δ*957-958* recovered in *E. coli* XL1-Blue
704 (ANG4741). The plasmid was shuttled through *E. coli* IM08B (ANG4743), introduced into *S. aureus*
705 LAC* (ANG4745) and following the allelic exchange procedure yielding the *S. aureus* strain
706 LAC*Δ*957-958* (*lcpB*) (ANG4749).
707 The plasmid pIMAY-Δ*mgtE* was designed to contain up- and downstream regions of
708 *SAUSA300_0910* (*mgtE*) fused together by the first and last 30 bp of the gene in order to create a
709 LAC*Δ*mgtE* mutant. For this, primer pairs P2374/P2375 and P2376/P2377 were used to amplify up-
710 and downstream regions and subsequently spliced together by PCR using primers P2374/P2377.
711 The PCR fragment was digested with XmaI/EcoRI and ligated into pIMAY cut with the same enzymes.
712 The plasmid pIMAY-Δ*mgtE* was recovered in *E. coli* XL1-Blue yielding strain ANG4146 and shuttled
713 through *E. coli* IM08B yielding strain ANG4158. The plasmid pIMAY-Δ*mgtE* was then introduced into
714 LAC* yielding strain LAC*Δ*SAUSA300_0910* (*mgtE*) (ANG4422) after the knockout procedure. To
715 create an empty vector-containing control strain and a plasmid-based complementation strain, the
716 plasmid piTET and piTET-*910* from strains ANG4163 and ANG4155 were isolated and used to
717 transform strain LAC*Δ*SAUSA300_0910* (*mgtE*) (ANG4422), yielding strains ANG4445 (LAC*Δ*mgtE*
718 piTET) and ANG4446 (LAC*Δ*mgtE* piTET-*mgtE)*.

719 The *tagO* gene (*SAUSA300_0731*) was inactivated using the targetron intron homing system (Yao *et*
720 *al.* 2006) or by allelic exchange using pIMAY* (Schuster *et al.* 2019). For the targetron mutagenesis,
721 plasmid pNL9164-*tagO* was produced by amplifying the upstream targetron fragment with primers
722 P2887 and the EBS universal primer (P2890) and the downstream fragment using primers
723 P2888/P2889, the fragments were fused using the IBS primer (P2887) and the EBS1d primer (P2888).
724 The final fragment was cloned using HindIII/BsrGI into pNL9164 (Yao *et al.* 2006). Plasmid pNL9164-
725 *tagO* was recovered in *E. coli* XL1-Blue, yielding strain ANG4703, introduced into *E. coli* IM08B to
726 give rise to strain ANG4704 and finally introduced into *S. aureus* LAC* (Boles *et al.* 2010) to create
727 strain LAC* pNL9164-*tagO* (ANG4751). The final *tagO* targetron mutant strain LAC**tagO*::targetron
728 (ANG4753) was generated using the method described by Yao *et al.* (Yao *et al.* 2006). For the
729 construction of *S. aureus* strain LAC*Δ*tagO* with an in-frame deletion in *tagO,* the allelic exchange
730 plasmid pIMAY*-Δ*tagO* was used. To this end, up- and downstream *tagO* fragments were produced
731 using primer pairs P2883/P2884 and P2885/P2886 and introduced by Gibson cloning into
732 XmaI/EcoRI pre-cut pIMAY*. Plasmid pIMAY*-Δ*tagO* was recovered in *E. coli* XL1-Blue, generating
733 strain ANG4755. After shuttling through *E. coli* strain IM08B (ANG4756), the plasmid was introduced
734 into *S. aureus* LAC* to create strain ANG4757. Finally, the *tagO* locus was deleted by allelic exchange,
735 generating strain LAC*Δ*tagO* (ANG4759). Because initial generation of the mutant failed, cells were
736 plated unselectively onto TSA plates and incubated at room temperature (18-25°C) for about two
737 weeks to enable colony differentiation between WT and Δ*tagO* mutant strains. Upon prolonged
738 incubation, *tagO* mutant strain colonies have an opaque appearance.

739 **Data access**

740 The whole genome sequencing data were deposited at the European Nucleotide Archive (ENA)
741 under accession id ERP115099 and TN-seq data in the short read archive (SRA) at the National

742 Center for Biotechnology Information (NCBI) under BioProject ID PRJNA544248. Analyzed tables can
743 be found in the supplementary files. For other data, please contact the corresponding author.

744 **Acknowledgements**

745 This research was funded by the Wellcome Trust through grants 100289 and 210671/Z/18/Z to A.G.
746 and the NIH grant P01AI083214 to S.W.. C.F.S. is funded by the German Research Foundation
747 [Deutsche Forschungsgemeinschaft (DFG)] through grant SCHU 3159/1–1 and F.C.M.K. was
748 supported by a Wellcome trust Ph.D. studentship. We thank Microbes NG and the London Institute
749 of Medical Sciences for providing whole genome sequencing services and the Tufts sequencing
750 facility for the sequencing services for the TN-seq experiments. We also would like to thank Ute
751 Bertsche for kind advice on HPLC analyses.

752 **Author contributions**

753 C.F.S., D.M.W., F.C.K. and A.G. performed the research; C.F.S., D.M.W., F.C.M.K., M.S., S.W. and A.G.
754 analyzed the data; C.F.S. and A.G. designed the research; C.F.S. and A.G. wrote the paper. All authors
755 approved the final version of the manuscript.

756 **Disclosure declaration**

757 The authors declare not conflict of interest.

758

759 **References**

760 Adams MR, Moss MO. 2008. 7.14.2 The Organism and its Characteristics. In *Food Microbiology (3rd*
761 *Edition)*. Royal Society of Chemistry.
762 Anderson CB, Witter LD. 1982. Glutamine and proline accumulation by *Staphylococcus aureus* with
763 reduction in water activity. *Appl Environ Microbiol* **43**: 1501-1503.

764 Atilano ML, Pereira PM, Vaz F, Catalão MJ, Reed P, Grilo IR, Sobral RG, Ligoxygakis P, Pinho MG,
765 Filipe SR. 2014. Bacterial autolysins trim cell surface peptidoglycan to prevent detection by
766 the *Drosophila* innate immune system. *Elife* **3**: e02277.
767 Bae JH, Miller KJ. 1992. Identification of two proline transport systems in *Staphylococcus aureus* and
768 their possible roles in osmoregulation. *Appl Environ Microbiol* **58**: 471-475.
769 Berger-Bächi B, Barberis-Maino L, Strässle A, Kayser FH. 1989. FemA, a host-mediated factor
770 essential for methicillin resistance in *Staphylococcus aureus*: molecular cloning and
771 characterization. *Mol Gen Genet* **219**: 263-269.
772 Boles BR, Thoendel M, Roth AJ, Horswill AR. 2010. Identification of genes involved in polysaccharide-
773 independent *Staphylococcus aureus* biofilm formation. *PLoS One* **5**: e10146.
774 Bowman L, Zeden MS, Schuster CF, Kaever V, Grundling A. 2016. New Insights into the Cyclic Di-
775 adenosine Monophosphate (c-di-AMP) Degradation Pathway and the Requirement of the
776 Cyclic Dinucleotide for Acid Stress Resistance in *Staphylococcus aureus*. *J Biol Chem* **291**:
777 26970-26986.
778 Brown S, Santa Maria JP, Jr., Walker S. 2013. Wall teichoic acids of gram-positive bacteria. *Annu Rev*
779 *Microbiol* **67**: 313-336.
780 Chan YG, Frankel MB, Dengler V, Schneewind O, Missiakas D. 2013. *Staphylococcus aureus* mutants
781 lacking the LytR-CpsA-Psr family of enzymes release cell wall teichoic acids into the
782 extracellular medium. *J Bacteriol* **195**: 4650-4659.
783 Chan YG, Kim HK, Schneewind O, Missiakas D. 2014. The capsular polysaccharide of *Staphylococcus*
784 *aureus* is attached to peptidoglycan by the LytR-CpsA-Psr (LCP) family of enzymes. *J Biol*
785 *Chem* **289**: 15680-15690.
786 Christian JH, Waltho JA. 1964. The Composition of *Staphylococcus aureus* in Relation to the Water
787 Activity of the Growth Medium. *J Gen Microbiol* **35**: 205-213.
788 Coe KA, Lee W, Komazin-Meredith G, Meredith TC, Grad YH, Walker S. 2019. Comparative Tn-Seq
789 reveals common daptomycin resistance determinants in *Staphylococcus aureus* despite
790 strain-dependent differences in essentiality of shared cell envelope genes. *bioRxiv*
791 doi:10.1101/648246: 648246.
792 Corrigan RM, Abbott JC, Burhenne H, Kaever V, Gründling A. 2011. c-di-AMP is a new second
793 messenger in *Staphylococcus aureus* with a role in controlling cell size and envelope stress.
794 *PLoS Pathog* **7**: e1002217.
795 Covas G, Vaz F, Henriques G, Pinho MG, Filipe SR. 2016. Analysis of Cell Wall Teichoic Acids in
796 *Staphylococcus aureus*. *Methods Mol Biol* **1440**: 201-213.
797 Csonka LN. 1989. Physiological and genetic responses of bacteria to osmotic stress. *Microbiol Rev*
798 **53**: 121-147.
799 Csonka LN, Hanson AD. 1991. Prokaryotic osmoregulation: genetics and physiology. *Annu Rev*
800 *Microbiol* **45**: 569-606.
801 de Jonge BL, Chang YS, Gage D, Tomasz A. 1992. Peptidoglycan composition of a highly methicillin-
802 resistant *Staphylococcus aureus* strain. The role of penicillin binding protein 2A. *J Biol Chem*
803 **267**: 11248-11254.
804 Fey PD, Endres JL, Yajjala VK, Widhelm TJ, Boissy RJ, Bose JL, Bayles KW. 2013. A genetic resource
805 for rapid and comprehensive phenotype screening of nonessential *Staphylococcus aureus*
806 genes. *MBio* **4**: e00537-00512.
807 Graham JE, Wilkinson BJ. 1992. *Staphylococcus aureus* osmoregulation: roles for choline, glycine
808 betaine, proline, and taurine. *J Bacteriol* **174**: 2711-2716.
809 Gründling A, Schneewind O. 2007. Genes required for glycolipid synthesis and lipoteichoic acid
810 anchoring in *Staphylococcus aureus*. *J Bacteriol* **189**: 2521-2530.
811 Holland LM, Conlon B, O'Gara JP. 2011. Mutation of *tagO* reveals an essential role for wall teichoic
812 acids in *Staphylococcus epidermidis* biofilm development. *Microbiology* **157**: 408-418.

813 Ishibashi M, Kurokawa K, Nishida S, Ueno K, Matsuo M, Sekimizu K. 2007. Isolation of temperature-
814 sensitive mutations in *murC* of *Staphylococcus aureus*. *FEMS Microbiology Letters* **274**: 204-
815 209.
816 Kho K, Meredith TC. 2018. Salt-Induced Stress Stimulates a Lipoteichoic Acid-Specific Three-
817 Component Glycosylation System in *Staphylococcus aureus*. *J Bacteriol* **200**.
818 Koprivnjak T, Mlakar V, Swanson L, Fournier B, Peschel A, Weiss JP. 2006. Cation-induced
819 transcriptional regulation of the dlt operon of *Staphylococcus aureus*. *J Bacteriol* **188**: 3622-
820 3630.
821 Lee CY, Buranen SL, Ye ZH. 1991. Construction of single-copy integration vectors for *Staphylococcus*
822 *aureus*. *Gene* **103**: 101-105.
823 Liebermeister W, Noor E, Flamholz A, Davidi D, Bernhardt J, Milo R. 2014. Visual account of protein
824 investment in cellular functions. *Proc Natl Acad Sci U S A* **111**: 8488-8493.
825 Lovering AL, De Castro L, Strynadka NC. 2008. Identification of dynamic structural motifs involved in
826 peptidoglycan glycosyltransfer. *J Mol Biol* **383**: 167-177.
827 Mäder U, Nicolas P, Depke M, Pané-Farré J, Debarbouille M, van der Kooi-Pol MM, Guérin C,
828 Dérozier S, Hiron A, Jarmer H et al. 2016. *Staphylococcus aureus* Transcriptome Architecture:
829 From Laboratory to Infection-Mimicking Conditions. *PLoS Genet* **12**: e1005962.
830 Madiraju MV, Brunner DP, Wilkinson BJ. 1987. Effects of temperature, NaCl, and methicillin on
831 penicillin-binding proteins, growth, peptidoglycan synthesis, and autolysis in methicillin-
832 resistant *Staphylococcus aureus*. *Antimicrob Agents Chemother* **31**: 1727-1733.
833 Mayer S, Steffen W, Steuber J, Götz F. 2015. The *Staphylococcus aureus* NuoL-like protein MpsA
834 contributes to the generation of membrane potential. *J Bacteriol* **197**: 794-806.
835 Measures JC. 1975. Role of amino acids in osmoregulation of non-halophilic bacteria. *Nature* **257**:
836 398-400.
837 Miller KJ, Zelt SC, Bae J-H. 1991. Glycine betaine and proline are the principal compatible solutes of
838 *Staphylococcus aureus*. *Current Microbiology* **23**: 131-137.
839 Mistretta N, Brossaud M, Telles F, Sanchez V, Talaga P, Rokbi B. 2019. Glycosylation of
840 *Staphylococcus aureus* cell wall teichoic acid is influenced by environmental conditions. *Sci*
841 *Rep* **9**: 3212.
842 Mitchell P, Moyle J. 1959. Permeability of the envelopes of *Staphylococcus aureus* to some salts,
843 amino acids, and non-electrolytes. *J Gen Microbiol* **20**: 434-441.
844 Mlynek KD, Callahan MT, Shimkevitch AV, Farmer JT, Endres JL, Marchand M, Bayles KW, Horswill
845 AR, Kaplan JB. 2016. Effects of Low-Dose Amoxicillin on *Staphylococcus aureus* USA300
846 Biofilms. *Antimicrob Agents Chemother* **60**: 2639-2651.
847 Monk IR, Shah IM, Xu M, Tan MW, Foster TJ. 2012. Transforming the untransformable: application
848 of direct transformation to manipulate genetically *Staphylococcus aureus* and
849 *Staphylococcus epidermidis*. *MBio* **3**.
850 Murakami K, Fujimura T, Doi M. 1994. Nucleotide sequence of the structural gene for the penicillin-
851 binding protein 2 of *Staphylococcus aureus* and the presence of a homologous gene in other
852 staphylococci. *FEMS Microbiol Lett* **117**: 131-136.
853 Ochiai T. 2000. *Staphylococcus aureus* produces autolysin-susceptible cell walls during growth in a
854 high-NaCl and low-Ca2+ concentration medium. *Microbiol Immunol* **44**: 97-104.
855 Onyango LA, Hugh Dunstan R, Roberts TK, Macdonald MM, Gottfries J. 2013. Phenotypic variants of
856 staphylococci and their underlying population distributions following exposure to stress.
857 *PLoS One* **8**: e77614.
858 Oshida T, Sugai M, Komatsuzawa H, Hong YM, Suginaka H, Tomasz A. 1995. A *Staphylococcus aureus*
859 autolysin that has an N-acetylmuramoyl-L-alanine amidase domain and an endo-beta-N-
860 acetylglucosaminidase domain: cloning, sequence analysis, and characterization. *Proc Natl*
861 *Acad Sci U S A* **92**: 285-289.

862 Ostash B, Walker S. 2010. Moenomycin family antibiotics: chemical synthesis, biosynthesis, and
863 biological activity. *Nat Prod Rep* **27**: 1594-1617.
864 Otto A, Bernhardt J, Meyer H, Schaffer M, Herbst FA, Siebourg J, Mäder U, Lalk M, Hecker M, Becher
865 D. 2010. Systems-wide temporal proteomic profiling in glucose-starved Bacillus subtilis. *Nat*
866 *Commun* **1**: 137.
867 Over B, Heusser R, McCallum N, Schulthess B, Kupferschmied P, Gaiani JM, Sifri CD, Berger-Bächi B,
868 Stutzmann Meier P. 2011. LytR-CpsA-Psr proteins in *Staphylococcus aureus* display partial
869 functional redundancy and the deletion of all three severely impairs septum placement and
870 cell separation. *FEMS Microbiol Lett* **320**: 142-151.
871 Pinho MG, Filipe SR, de Lencastre H, Tomasz A. 2001. Complementation of the essential
872 peptidoglycan transpeptidase function of penicillin-binding protein 2 (PBP2) by the drug
873 resistance protein PBP2A in *Staphylococcus aureus*. *J Bacteriol* **183**: 6525-6531.
874 Pöhlmann-Dietze P, Ulrich M, Kiser KB, Döring G, Lee JC, Fournier JM, Botzenhart K, Wolz C. 2000.
875 Adherence of *Staphylococcus aureus* to endothelial cells: influence of capsular
876 polysaccharide, global regulator agr, and bacterial growth phase. *Infect Immun* **68**: 4865-
877 4871.
878 Pourkomailian B, Booth IR. 1992. Glycine betaine transport by *Staphylococcus aureus*: evidence for
879 feedback regulation of the activity of the two transport systems. *Microbiology* **140 (Pt 11)**:
880 3131-3138.
881 Price-Whelan A, Poon CK, Benson MA, Eidem TT, Roux CM, Boyd JM, Dunman PM, Torres VJ,
882 Krulwich TA. 2013. Transcriptional profiling of *Staphylococcus aureus* during growth in 2 M
883 NaCl leads to clarification of physiological roles for Kdp and Ktr K+ uptake systems. *MBio* **4**.
884 Rahman MM, Hunter HN, Prova S, Verma V, Qamar A, Golemi-Kotra D. 2016. The *Staphylococcus*
885 *aureus* Methicillin Resistance Factor FmtA Is a d-Amino Esterase That Acts on Teichoic Acids.
886 *MBio* **7**: e02070-02015.
887 Santiago M, Matano LM, Moussa SH, Gilmore MS, Walker S, Meredith TC. 2015. A new platform for
888 ultra-high density *Staphylococcus aureus* transposon libraries. *BMC Genomics* **16**: 252.
889 Schaefer K, Matano LM, Qiao Y, Kahne D, Walker S. 2017. In vitro reconstitution demonstrates the
890 cell wall ligase activity of LCP proteins. *Nat Chem Biol* **13**: 396-401.
891 Schindelin J, Arganda-Carreras I, Frise E, Kaynig V, Longair M, Pietzsch T, Preibisch S, Rueden C,
892 Saalfeld S, Schmid B et al. 2012. Fiji: an open-source platform for biological-image analysis.
893 *Nat Methods* **9**: 676-682.
894 Schuster CF, Bertram R. 2014. Fluorescence based primer extension technique to determine
895 transcriptional starting points and cleavage sites of RNases *in vivo*. *J Vis Exp*
896 doi:10.3791/52134: e52134.
897 Schuster CF, Howard SA, Gründling A. 2019. Use of the counter selectable marker PheS* for genome
898 engineering in *Staphylococcus aureus*. *Microbiology* doi:10.1099/mic.0.000791.
899 Schwan WR, Lehmann L, McCormick J. 2006. Transcriptional activation of the *Staphylococcus aureus*
900 putP gene by low-proline-high osmotic conditions and during infection of murine and human
901 tissues. *Infect Immun* **74**: 399-409.
902 Scybert S, Pechous R, Sitthisak S, Nadakavukaren MJ, Wilkinson BJ, Jayaswal RK. 2003. NaCl-sensitive
903 mutant of *Staphylococcus aureus* has a Tn917-lacZ insertion in its ars operon. *FEMS Microbiol*
904 *Lett* **222**: 171-176.
905 Sleator RD, Hill C. 2002. Bacterial osmoadaptation: the role of osmolytes in bacterial stress and
906 virulence. *FEMS Microbiol Rev* **26**: 49-71.
907 Stapleton MR, Horsburgh MJ, Hayhurst EJ, Wright L, Jonsson IM, Tarkowski A, Kokai-Kun JF, Mond
908 JJ, Foster SJ. 2007. Characterization of IsaA and SceD, two putative lytic transglycosylases of
909 *Staphylococcus aureus*. *J Bacteriol* **189**: 7316-7325.

910 Stewart CM, Cole MB, Legan JD, Slade L, Schaffner DW. 2005. Solute-specific effects of osmotic
911 stress on *Staphylococcus aureus*. *J Appl Microbiol* **98**: 193-202.
912 Stewart CM, Cole MB, Legan JD, Slade L, Vandeven MH, Schaffner DW. 2002. *Staphylococcus aureus*
913 growth boundaries: moving towards mechanistic predictive models based on solute-specific
914 effects. *Appl Environ Microbiol* **68**: 1864-1871.
915 Tong SY, Davis JS, Eichenberger E, Holland TL, Fowler VG, Jr. 2015. *Staphylococcus aureus* infections:
916 epidemiology, pathophysiology, clinical manifestations, and management. *Clin Microbiol Rev*
917 **28**: 603-661.
918 Townsend DE, Wilkinson BJ. 1992. Proline transport in *Staphylococcus aureus*: a high-affinity system
919 and a low-affinity system involved in osmoregulation. *J Bacteriol* **174**: 2702-2710.
920 Vaish M, Price-Whelan A, Reyes-Robles T, Liu J, Jereen A, Christie S, Alonzo F, 3rd, Benson MA, Torres
921 VJ, Krulwich TA. 2018. Roles of *Staphylococcus aureus* Mnh1 and Mnh2 Antiporters in Salt
922 Tolerance, Alkali Tolerance, and Pathogenesis. *J Bacteriol* **200**.
923 Vijaranakul U, Nadakavukaren MJ, de Jonge BL, Wilkinson BJ, Jayaswal RK. 1995. Increased cell size
924 and shortened peptidoglycan interpeptide bridge of NaCl-stressed *Staphylococcus aureus*
925 and their reversal by glycine betaine. *J Bacteriol* **177**: 5116-5121.
926 Vijaranakul U, Xiong A, Lockwood K, Jayaswal RK. 1998. Cloning and nucleotide sequencing of a
927 *Staphylococcus aureus* gene encoding a branched-chain-amino-acid transporter. *Appl*
928 *Environ Microbiol* **64**: 763-767.
929 Vollmer W, Blanot D, de Pedro MA. 2008. Peptidoglycan structure and architecture. *FEMS Microbiol*
930 *Rev* **32**: 149-167.
931 Wengender PA, Miller KJ. 1995. Identification of a PutP proline permease gene homolog from
932 *Staphylococcus aureus* by expression cloning of the high-affinity proline transport system in
933 Escherichia coli. *Appl Environ Microbiol* **61**: 252-259.
934 Wertheim HF, Melles DC, Vos MC, van Leeuwen W, van Belkum A, Verbrugh HA, Nouwen JL. 2005.
935 The role of nasal carriage in *Staphylococcus aureus* infections. *Lancet Infect Dis* **5**: 751-762.
936 Wetzel KJ, Bjorge D, Schwan WR. 2011. Mutational and transcriptional analyses of the
937 *Staphylococcus aureus* low-affinity proline transporter OpuD during *in vitro* growth and
938 infection of murine tissues. *FEMS Immunol Med Microbiol* **61**: 346-355.
939 Wyke AW. 1984. Isolation of five penicillin-binding proteins from *Staphylococcus aureus*. *FEMS*
940 *Microbiology Letters* **22**: 133-138.
941 Yao J, Zhong J, Fang Y, Geisinger E, Novick RP, Lambowitz AM. 2006. Use of targetrons to disrupt
942 essential and nonessential genes in *Staphylococcus aureus* reveals temperature sensitivity
943 of Ll.LtrB group II intron splicing. *RNA* **12**: 1271-1281.
944 Zeden MS, Schuster CF, Bowman L, Zhong Q, Williams HD, Gründling A. 2018. Cyclic di-adenosine
945 monophosphate (c-di-AMP) is required for osmotic regulation in *Staphylococcus aureus* but
946 dispensable for viability in anaerobic conditions. *J Biol Chem* **293**: 3180-3200.
947

948

949 **Figure legends**

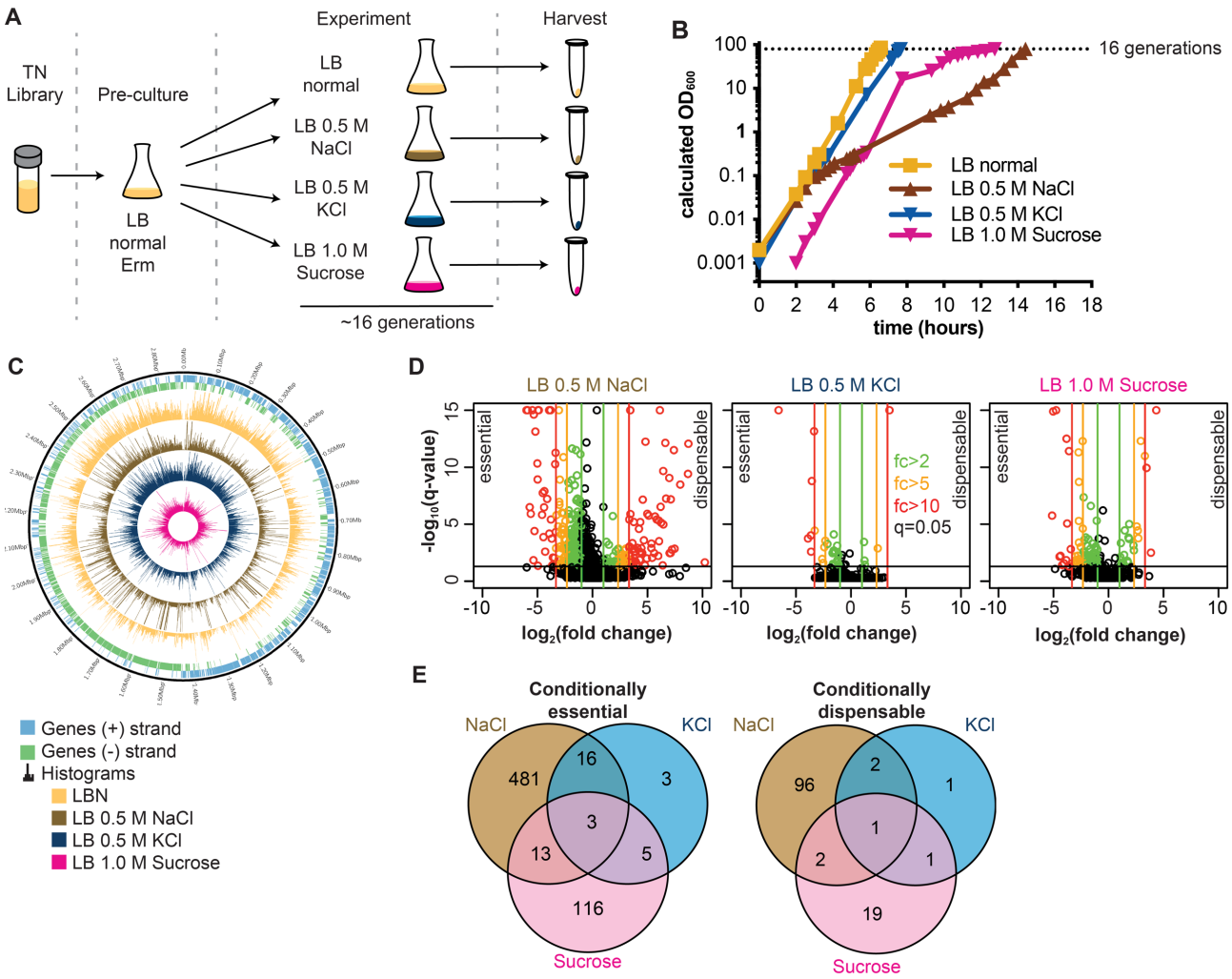

950

951 **Fig. 1. Different sets of genes are conditionally essential for the growth of *S. aureus* under NaCl,**

952 **KCl or sucrose stress conditions.**

953 (A) Workflow of the TN-seq experiment. A TN-seq library was pre-cultured and then used to

954 inoculate LBN, LB containing 0.5 M NaCl, 0.5 M KCl or 1 M sucrose. Cells were kept in exponential

955 phase for 16 generations, harvested and transposon insertion sites determined by high throughput

956 sequencing.

957 (B) Growth curves. For the TN-seq experiment (n=1), the growth of an *S. aureus* library cultured in

958 LBN, LB 0.5M NaCl, LB 0.5 M KCl or LB 1.0 M sucrose medium was followed by taking OD_{600}

959 measurements at timed intervals. The cultures were back-diluted once when they reached an OD_{600}

960 of approximately 0.3. The plotted OD_{600} values were calculated by multiplying the measured OD_{600}
961 with the dilution factor. The dotted line indicates the 16 generation cut-off at which cultures were
962 harvested.
963 (C) Circular plot showing the transposon insertion density along the *S. aureus* genome under
964 different osmotic stress conditions. The two outer rings depict genes located on the (+) or (-) strand
965 in *S. aureus* strain USA300 FPR3757. The inner four rings show the histograms of transposon
966 insertions on a per gene basis after growth of the library in LBN (orange), 0.5 M NaCl (brown), 0.5
967 M KCl (blue) and 1 M sucrose (pink) medium for 16 generations.
968 (D) Volcano plots of conditionally essential and dispensable genes following growth of *S. aureus* in
969 0.5 M NaCl, 0.5 M KCl or 1 M sucrose medium and compared to LBN conditions. q-values represent
970 Benjamini-Hochberg corrected p-values, and $\log_2$ (fold changes) indicate essential genes (negative
971 values) or dispensable genes (positive values). The black horizontal line indicates a q-value of 0.05,
972 which was deemed the significance level. Vertical lines indicate 2- (green), 5- (orange) or 10- (red)
973 fold changes in either direction. Each dot represents one gene and coloring follows the fold-change
974 scheme whenever the q-value threshold was met. Very small q-values were truncated to fit onto
975 the graph. The TN-seq experiments were conducted once (n=1).
976 (E) Venn diagrams showing overlaps of conditionally essential and dispensable genes during
977 prolonged NaCl, KCl or sucrose stress. Genes with a 2-fold decrease (essential genes) or a 2-fold
978 increase (dispensable genes) in transposon insertions under each stress condition compared to the
979 LBN condition and a q-value of ≤0.05 were determined and the overlap between these gene lists
980 displayed in Venn diagrams.
981

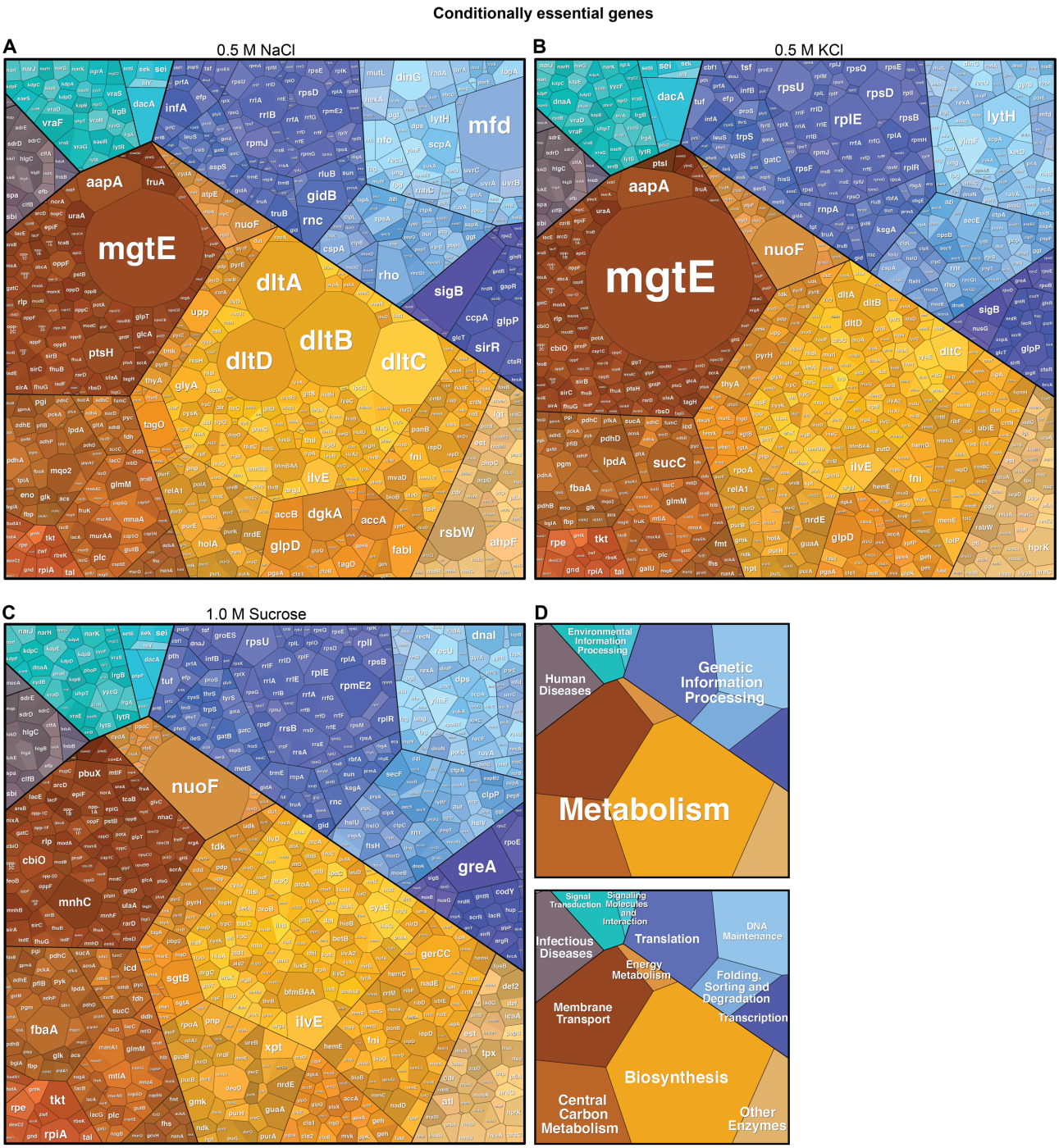

Fig. 2. Voronoi diagram-based visualization of conditionally essential *S. aureus* genes when exposed to different osmotic stressors underlines differences.

Conditionally essential genes of *S. aureus* strains grown either in 0.5 M NaCl (A), 0.5 M KCl (B) or 1.0 M sucrose (C) were mapped to cellular functions. Area sizes were adjusted to their essentiality regardless of p- or q-value to visualize differences on a genome wide level. The larger the area, the

988 higher the number of transposon insertions in the LBN control condition as compared to the stress

989 conditions. Colors of polygons indicate cellular functions as detailed in (D).

990

991

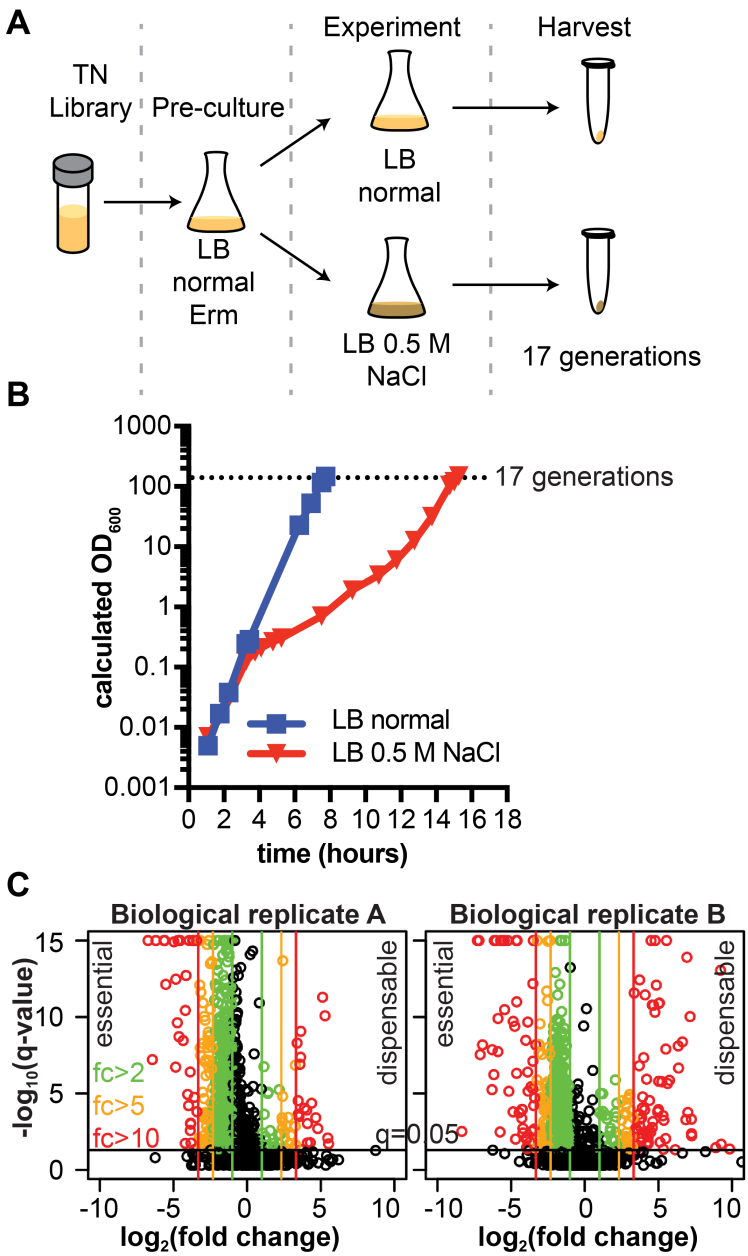

992

993 **Fig. 3. TN-Seq screen reveals essential and dispensable genes during prolonged NaCl stress in *S.***
994 ***aureus*.**

995 (A) Workflow of TN-seq experiments. A saturated transposon library was pre-cultured for one hour,

996 then used to inoculate LB medium containing either normal levels (0.086 M) or 0.5 M of NaCl. After

997 17 generations, cells were harvested, and transposon insertion sites determined by high throughput

998 sequencing.

999 (B) Growth curve. Growth of the *S. aureus* library culture in LBN and LB 0.5 M medium was followed
1000 by determining OD_{600} readings. Dotted line indicates 17 generation threshold. Cultures were back-
1001 diluted once when they reached an OD of approximately 0.3 and the optical densities shown are
1002 calculated from measured ODs time dilution factor. Culture from replicate B (n=1) is shown and a
1003 similar growth profile was seen for replicate A.
1004 (C) Volcano plots of essential and dispensable genes in NaCl conditions compared to LBN. Negative
1005 log_2 fold-changes indicate essential and positive log_2 fold-changes dispensable genes. q-value stands
1006 for Benjamini-Hochberg false discovery rate. Black horizontal line indicates q-value of 0.05 (cut-off)
1007 and red, orange and green vertical lines 10-, 5- and 2-fold differences in either direction. Colored
1008 circles indicate genes for which a significant change in the number of transposon insertions was
1009 observed above q-value cutoff and follow the same color code as the vertical lines. Very small q-
1010 values were truncated to fit onto the graph. Replicate A is shown in left panel and replicate B in right
1011 panel (n=1 for each plot).

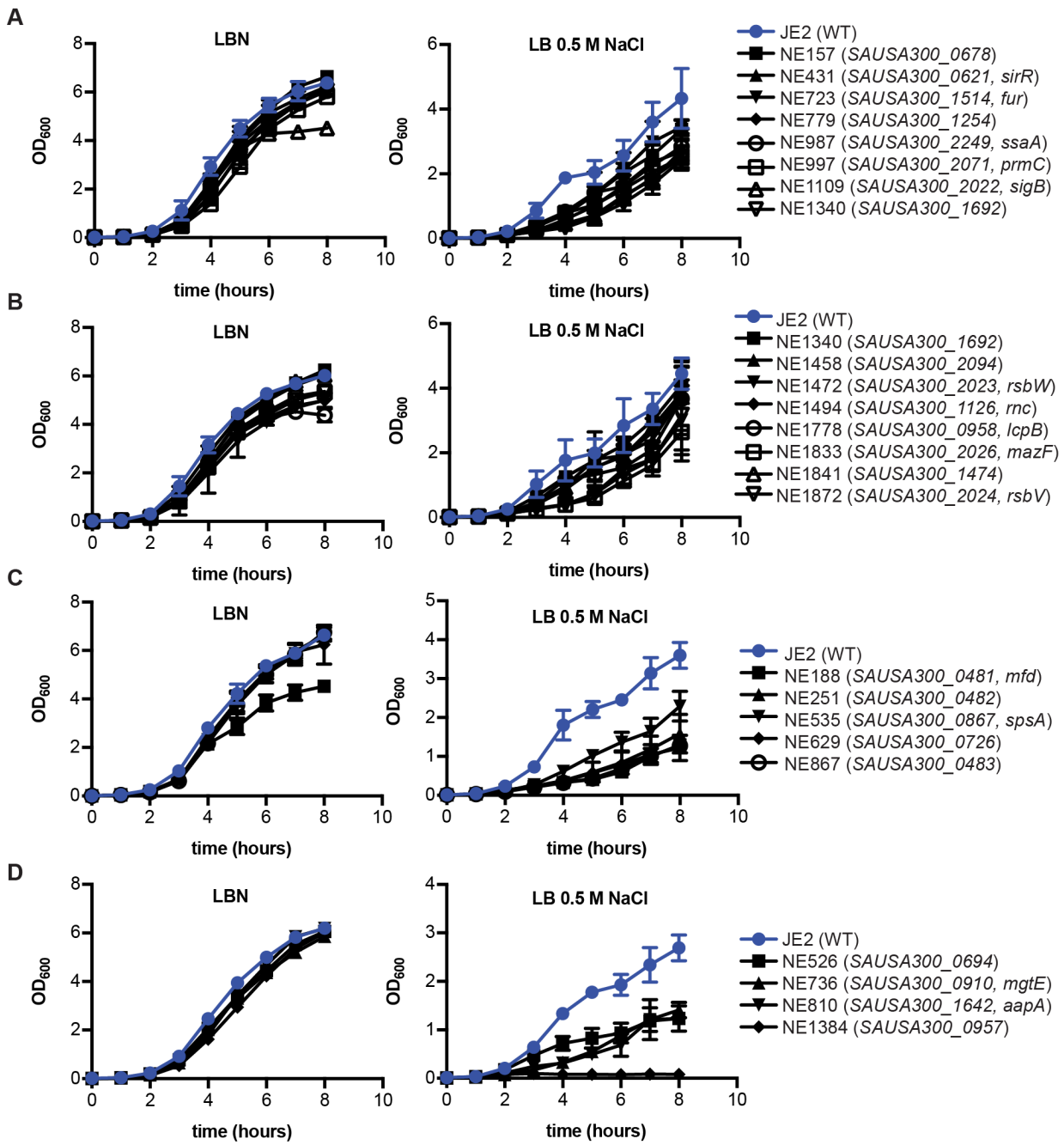

Fig. 4. Growth curves of *S. aureus* strains with transposon insertions in potential salt essential genes.

S. aureus strain JE2 (WT) and strains from the Nebraska Transposon Mutant Library (NTML) containing transposon insertions in potential salt essential genes were grown in LBN (left column) or 0.5 M NaCl LB medium (right column) and their growth monitored over 8 hours. Transposon mutant strains shown in panels (A) and (B) had a mild growth defect while strains shown in panels (C) and (D) had a stronger growth defect when grown in the high salt medium. NE numbers

1020 correspond to the NTML mutant number. Locus tag number and where available gene names with

1021 transposon insertion site are given in parenthesis. Growth curves were performed in triplicates

1022 (n=3) and means and SDs were plotted.

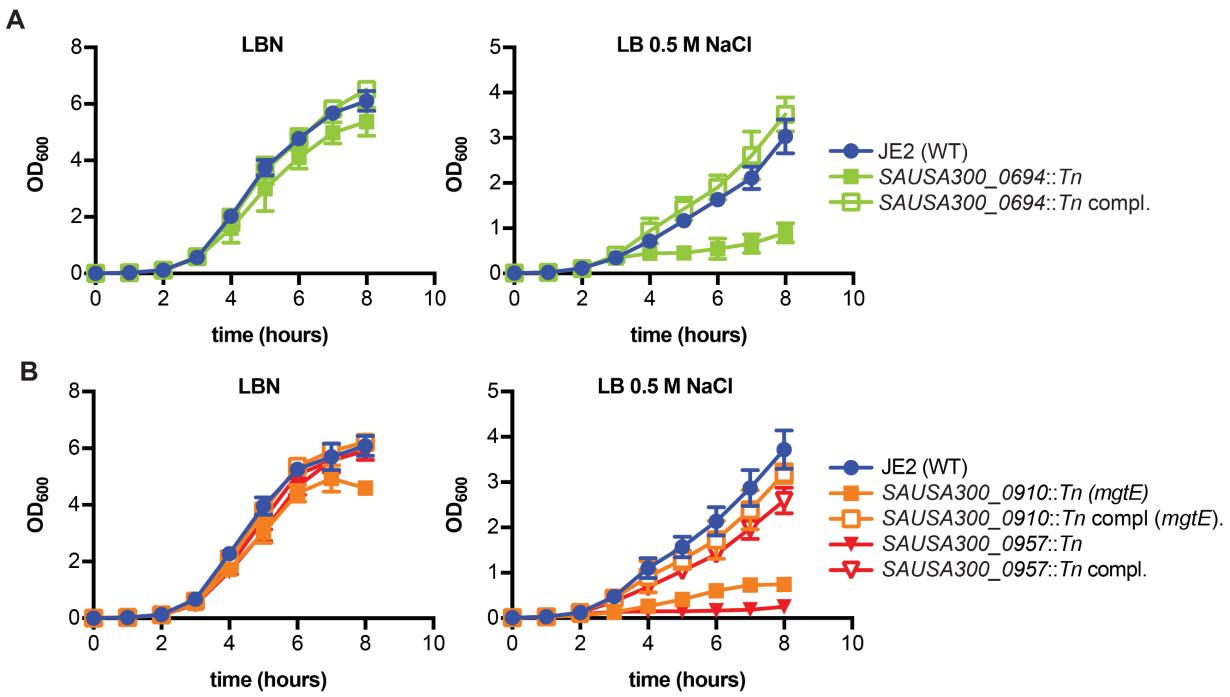

Fig. 5. Growth curves and complementation analysis of *S. aureus* strains with transposon insertions in salt essential genes.

S. aureus strains (A) JE2 (WT), *SAUSA300_0694::Tn* mutant with empty plasmid and complementation strain or (B) JE2 (WT), *SAUSA300_0910* (*mgtE*), *SAUSA300_0957::Tn* with empty plasmid and respective complementation strains were grown in LBN (left panels) or LB 0.5 M NaCl medium (right panels) supplemented with 100 ng/ml Atet and OD_{600} readings determined at timed intervals. Growth curves were performed in triplicates (n=3) and means and SDs of OD_{600} readings were plotted.

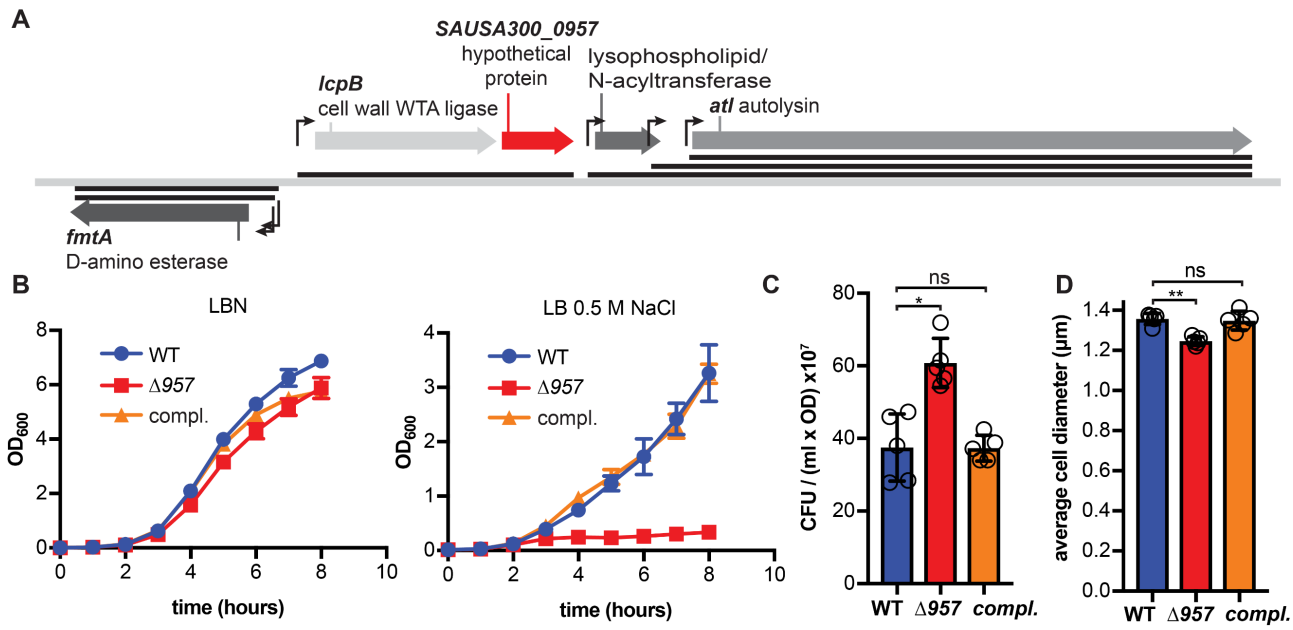

Fig. 6. Gene *SAUSA300_0957* is located in a genomic region with cell envelope genes and its deletion leads to salt sensitivity and other phenotypic changes.

(A) Schematic of the *S. aureus* USA300 FPR3757 chromosomal region with gene *SAUSA300_0957* (gene *957*). Gene *957* is encoded in an operon with *lcpB*, which codes for a wall teichoic acid ligase. *fmtA,* a proposed D-amino esterase acting on teichoic acid and genes coding for a predicted acyltransferase and the major autolysin Atl are located up and downstream of this operon. Putative promoters are shown as angled arrows (adapted from (Mäder *et al.* 2016)) and black bars indicate the corresponding transcripts.

(B) Growth curves. *S. aureus* strains LAC* piTET (WT), LAC*Δ*957* piTET (Δ*957*) and the complementation strain LAC*Δ*957* piTET-*957* (compl.) were grown in LBN or LB containing 0.5 M NaCl medium and 100 ng/ml Atet. The growth was monitored by determining OD_{600} readings the means and SDs from three independent experiments were plotted.

(C) Determination of CFU/OD ratios. OD_{600} values as well as CFU/ml were determined for overnight cultures of the *S. aureus* strains described in panel (B) and the means and SDs of the CFU per ml OD_{600} of 1 from five independent experiments were plotted.

1050 (D) Cell size measurements. The cell walls of the *S. aureus* strains described in panel (B) were stained
1051 with fluorescently labelled vancomycin and the cells subsequently observed under a microscope.
1052 The diameters of 200 cells were measured and the means calculated. This average of the means and
1053 SDs from five independent experiments were plotted.
1054 For statistical analysis, a Kruskal-Wallis one-way ANOVA test was performed followed by a Dunn's
1055 post-hoc test to determine p-values. Asterisks (*) indicate $p \leq 0.05$ and two asterisks (**) $p \leq 0.01$ and
1056 ns=not significant.
1057

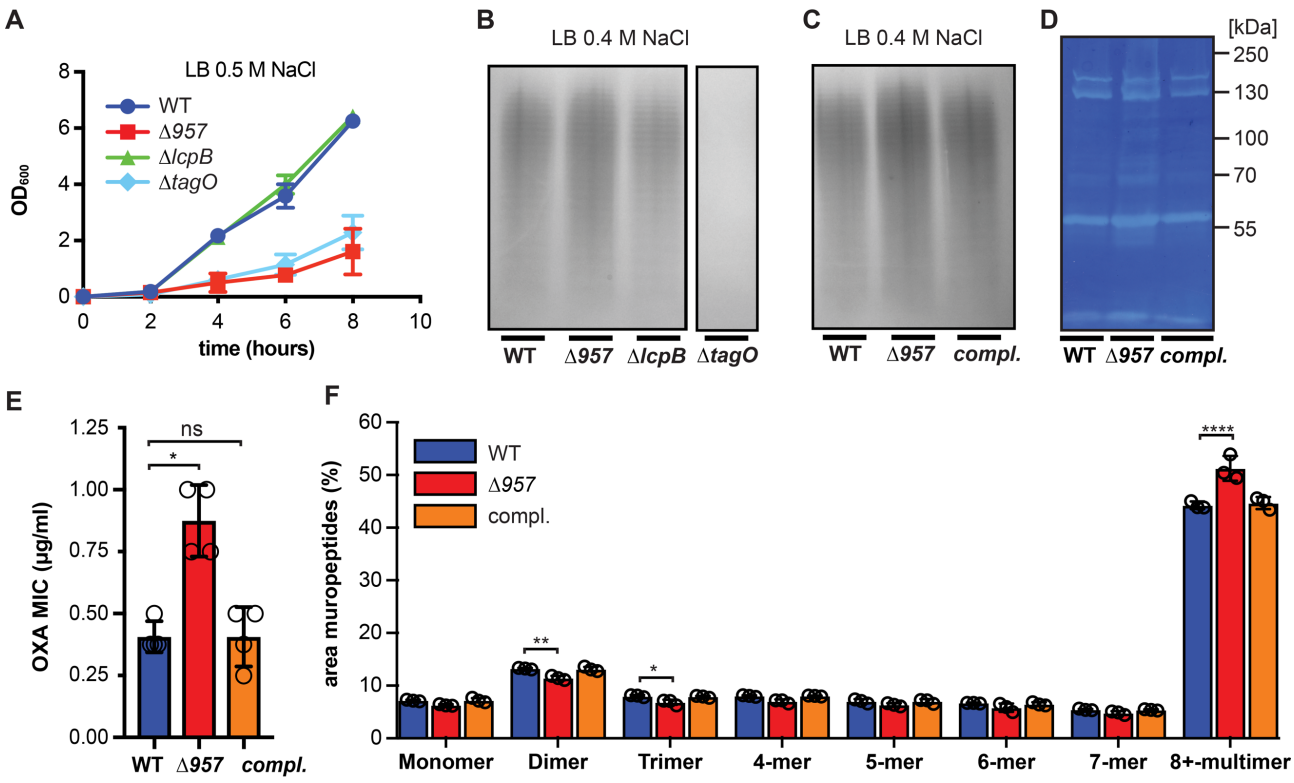

Fig. 7. Inactivation of gene 957 leads to an increase in peptidoglycan crosslinking.

(A) Growth curves. *S. aureus* strains LAC* (WT), LAC*Δ*957* (Δ*957*), LAC*Δ*lcpB*, (Δ*957*), and LAC*Δ*tagO* (Δ*tagO*) were grown in LB 0.5 M NaCl medium and OD_{600} readings determined at timed intervals. The means and SDs from three biological replicates were plotted.

(B) Detection of WTA on silver stained gels. WTA was isolated from *S. aureus* strains described in panel (A) following growth in LB 0.4 M NaCl medium. The WTA was separated by electrophoresis and visualized by silver stain. The experiment was performed three times and one representative gel image is shown.

(C) Detection of WTA on silver stained gels. Same as (B) but using the strains LAC* piTET (WT), LAC*Δ*957* piTET (Δ*957*), and the complementation strain LAC*Δ*957* piTET-*957* (compl.) grown in LB 0.4 M NaCl medium also containing 100 ng/ml Atet.

(D) Zymogram gel. Cell extracts prepared from *S. aureus* strains described in panel (C) were separated on a gel containing heat killed *Micrococcus luteus* cells. Autolysins were renatured and

1072 the zones of lysis visualized by methylene blue staining. The experiment was performed twice and
1073 one experiment is shown.
1074 (E) Determination of oxacillin MICs. Oxacillin MICs were determined for *S. aureus* strains described
1075 in panel (C) using Etest strips. The median and SDs from four biological replicates were plotted.
1076 (F) Muropeptide analysis. The same *S. aureus* strains as described in (C) were grown in LB 0.4 M
1077 NaCl medium also containing 100 ng/ml Atet, peptidoglycan isolated and digested with mutanolysin
1078 and the resulting muropeptide fragments separated by HPLC. Representative chromatograms are
1079 shown in Supplementary Figures S6E. The peak area of individual peaks (corresponding to monomer
1080 up to 8-mers and above) were quantified and the means and SDs from three biological replicates
1081 plotted.
1082 For statistical analysis of the oxacillin MICs in (E) a Kruskal-Wallis one-way ANOVA and a Dunn's
1083 post-hoc test was performed and for the muropeptide analysis in (F) a two-way ANOVA and a
1084 Dunnett's post-hoc test. One asterisk (*) indicates $p \leq 0.05$, two asterisks (**) $p \leq 0.01$ and four
1085 asterisks (****) $p \leq 0.0001$. ns=not significant.
1086

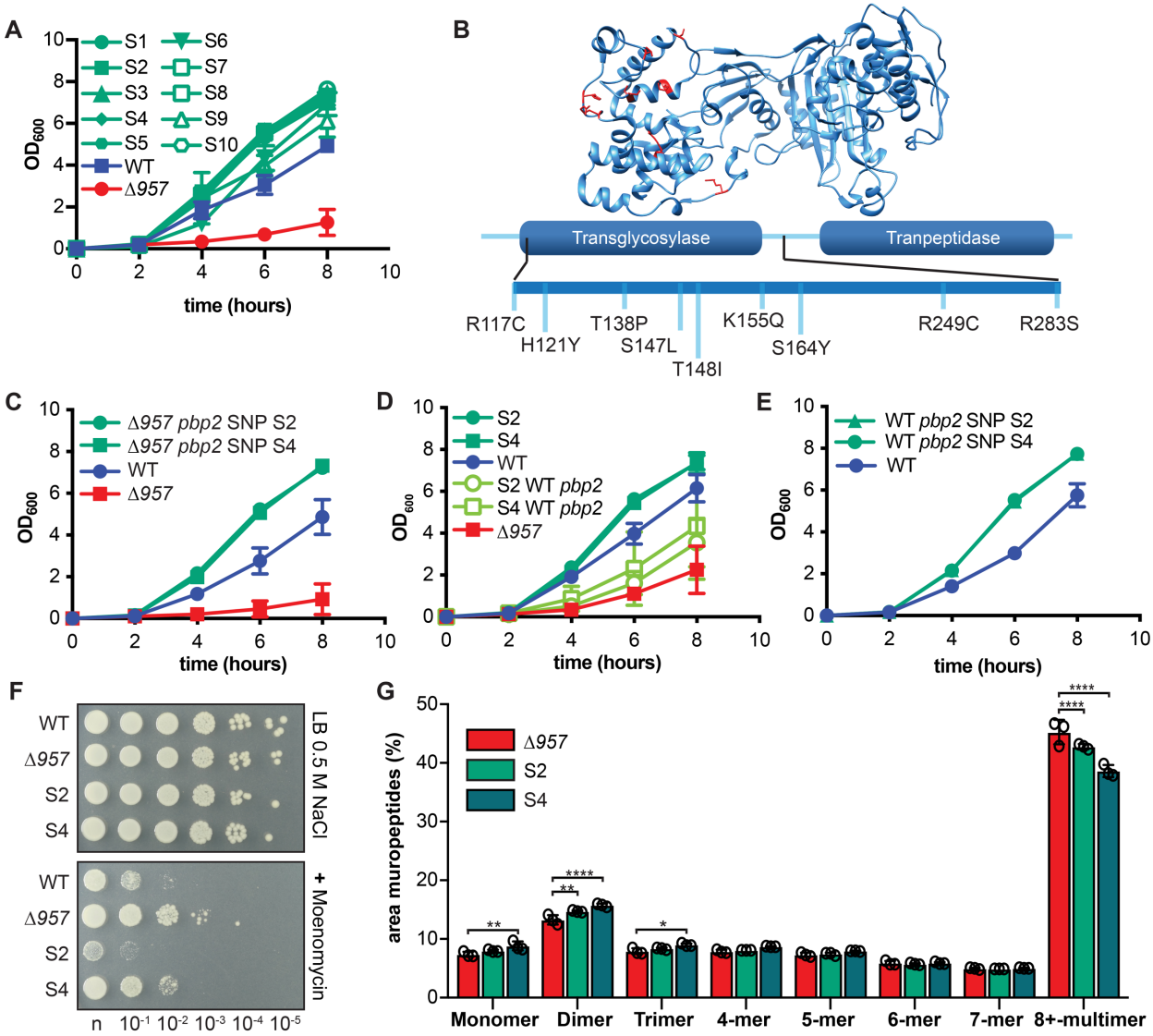

Fig. 8. The growth and peptidoglycan defect observed for the *957* mutant can be rescued by compensatory mutations in *pbp2*.

(A) Growth curves. *S. aureus* strains LAC* (WT), LAC*Δ*957* (Δ*957*) and the LAC*Δ*957* suppressors S1-10 (S1 to 10) were grown in LB 0.5 M NaCl medium, OD_{600} readings determined and the means and SDs of four biological replicates plotted.

(B) Schematic of Pbp2 with amino acid substitutions identified. Top: Structure of the *S. aureus* penicillin binding protein Pbp2 (PDB: 3DWK, (Lovering *et al.* 2008)) with amino acids that are altered in the obtained suppressor strains shown in red. Bottom: Schematic of the Pbp2 enzyme with the

1096 transglycosylase and transpeptidase domains as well as the observed amino acid changes in the
1097 transglycosylase domain indicated.
1098 (C) Growth curves using *957* mutant strains containing *pbp2* alleles from suppressors S2 and S4.
1099 Growth curves were performed in LB 0.5 M NaCl medium and plotted as described in panel (A) but
1100 using *S. aureus* strains LAC* *1332*::Tn (WT), LAC*Δ*957* *1332*::Tn (Δ*957*), LAC*Δ*957* *1332*::Tn *pbp2*
1101 SNP S2 (Δ*957* *pbp2* SNP S2), LAC*Δ*957* suppressor S4 *1332*::Tn (Δ*957* *pbp2* SNP S4).
1102 (D) Growth curves using *957* suppressors with their *pbp2* gene repaired to WT. Growth curves were
1103 performed in LB 0.5 M NaCl medium and plotted as described in panel (A) but using *S. aureus* strains
1104 LAC* *1332*::Tn (WT), LAC*Δ*957* *1332*::Tn (Δ*957*), LAC*Δ*957* suppressor S2 *1332*::Tn (S2), LAC*Δ*957*
1105 suppressor S4 *1332*::Tn (S4), LAC*Δ*957* suppressor S2 *1332*::Tn repaired WT *pbp2* (S2 WT *pbp2*),
1106 and LAC*Δ*957* suppressor S4 *1332*::Tn repaired WT *pbp2* (S4 WT *pbp2*).
1107 (E) Growth curves using WT strains carrying *pbp2* SNPs. *S. aureus* strains LAC* *1332*::Tn (WT), LAC*
1108 *1332*::Tn *pbp2* SNP S2 (WT *pbp2* SNP S2) and LAC* *1332*::Tn *pbp2* SNP S4 (WT *pbp2* SNP S4) were
1109 grown in LB 0.5 M NaCl medium and OD_{600} readings determined and the means and SDs of three
1110 biological replicates plotted.
1111 (F) Bacterial growth on moenomycin supplemented agar plates. *S. aureus* strains LAC* (WT),
1112 LAC*Δ*957* (Δ*957*), LAC*Δ*957* Suppressor S2 (S2) and S4 LAC*Δ*957* Suppressor S4 (S4) were grown
1113 to exponential phase, normalized to an OD_{600} of 0.1 and plated either neat (n) or in 10-fold dilutions
1114 onto LB agar containing 0.5 M NaCl without (top) or with (bottom) moenomycin. Shown is one
1115 representative image of three biological replicates.
1116 (G) Muropeptide analysis. *S. aureus* strains LAC*Δ*957* (Δ*957*), LAC*Δ*957* Suppressor S2 (S2) and S4
1117 LAC*Δ*957* Suppressor S4 (S4) were grown in 0.4 M NaCl LB medium and muropeptides quantified
1118 as described in Fig 5F. Representative chromatograms are shown in Supplementary Figure S8D. The
1119 means and SDs from three biological replicates were plotted. For statistical analysis a two-way

1120 ANOVA and Dunnett's post-hoc test was performed. One asterisk (*) indicates $p \leq 0.05$, two asterisks

1121 (**) $p \leq 0.01$ and four asterisks (****) $p \leq 0.0001$.

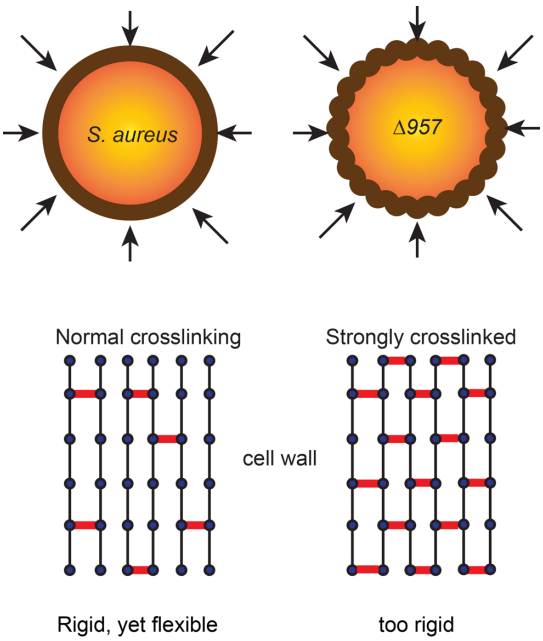

Fig. 9. Proposed model of 957 activity during NaCl stress.

S. aureus is normally able to grow in medium containing up to 2.5 M NaCl. The deletion of gene *957* leads to a strong growth defect in high salt conditions and changes in the peptidoglycan structure. We speculate that the observed increase in peptidoglycan crosslinking will lead to an increased rigidity of the cell wall and therefore increased cell wall damage when these cells are exposed to osmotic stress conditions.

Supplementary Figures

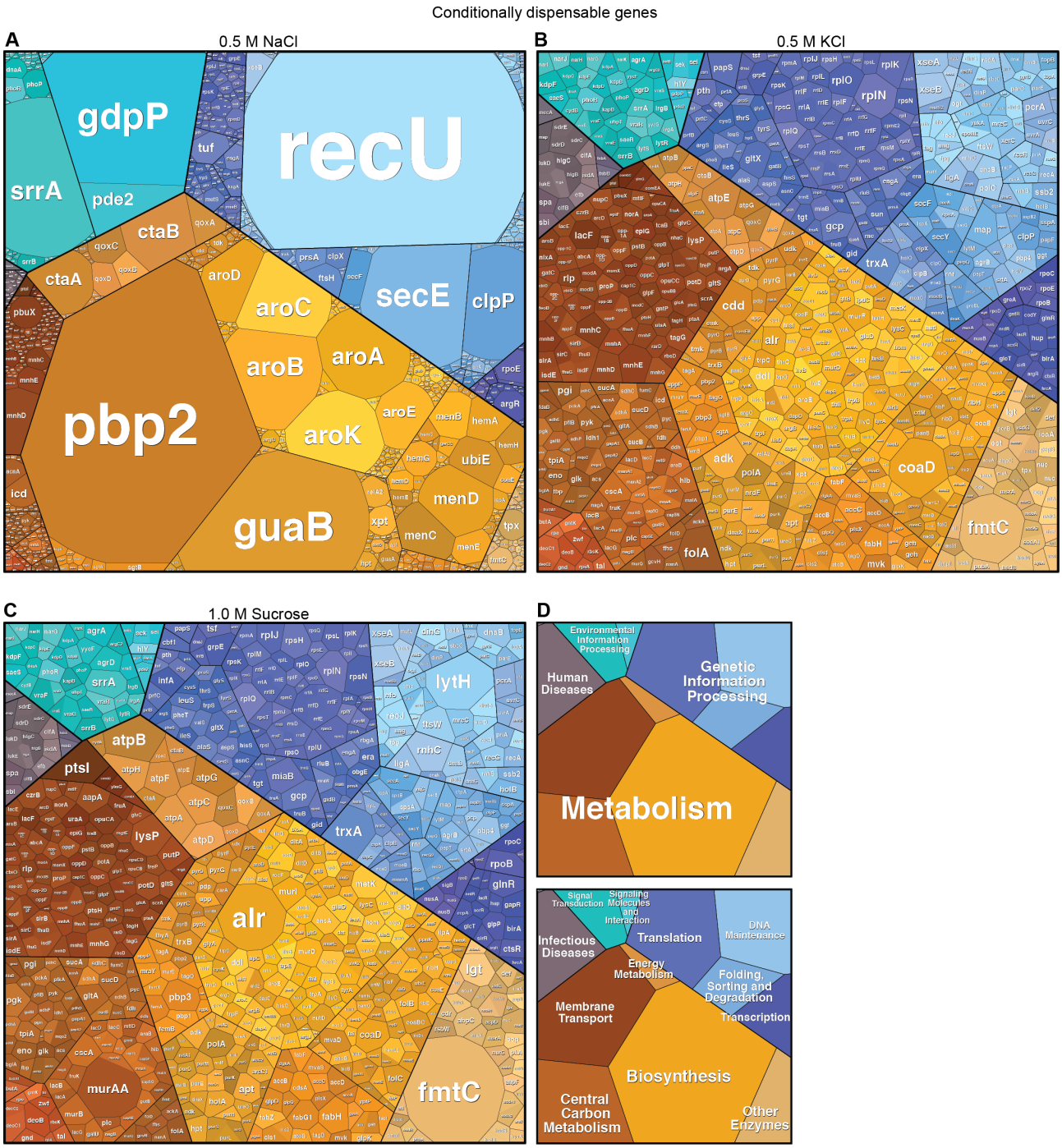

Supplementary Fig. 1. Voronoi diagram-based visualization of conditionally dispensable *S. aureus* genes when exposed to different osmotic stressors.

Conditionally dispensable genes of *S. aureus* strains grown either in 0.5 M NaCl (A), 0.5 M KCl (B) or 1.0 M sucrose (C) were mapped to cellular functions with area sizes adjusted to their essentiality

1136 regardless of p- or q-value. The larger the area, the higher the number of transposon insertions in

1137 relation to the LBN control. *recU* was scaled to 1/10 of the original ratio to preserve space. Colors

1138 of polygons indicate cellular functions as detailed in (D).

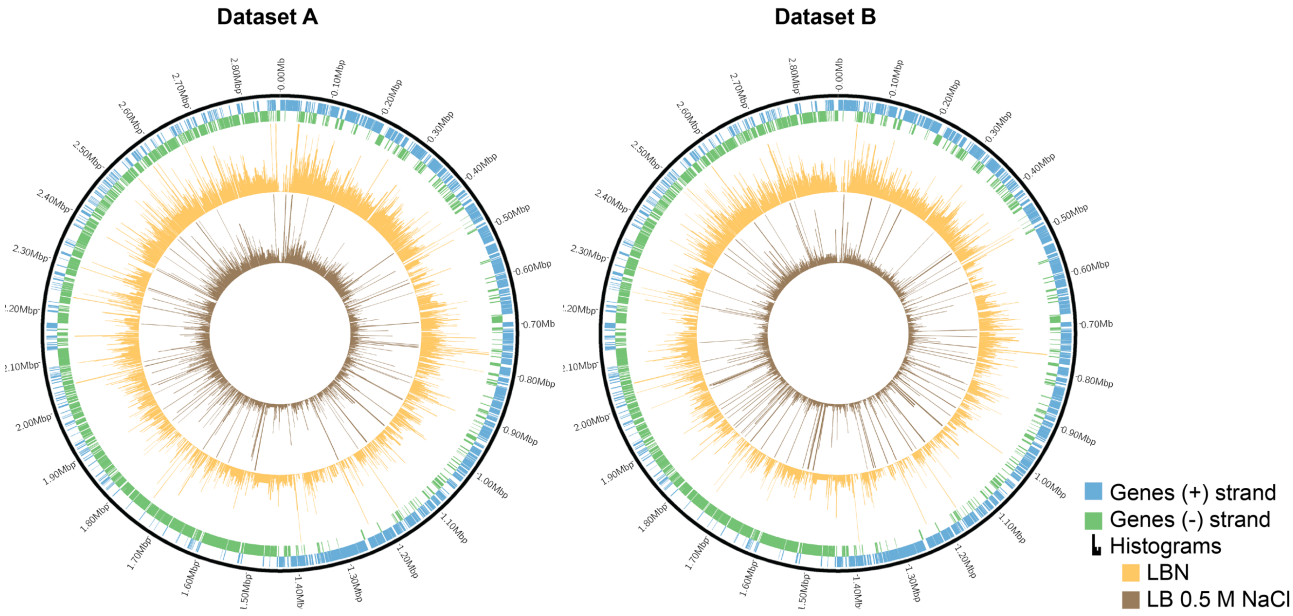

Supplementary Fig. 2. Circos plots showing transposon insertions in the *S. aureus* genome following growth under different conditions.

The outer two bands represent genes on the forward (blue) and reverse (green) strand, respectively. The inner three rings represent transposon insertions per gene following the growth of *S. aureus* in in either LBN (orange) or LB 0.5 M NaCl (brown) for 17 generations. Each circular plot represents one individual experiment (n=1).

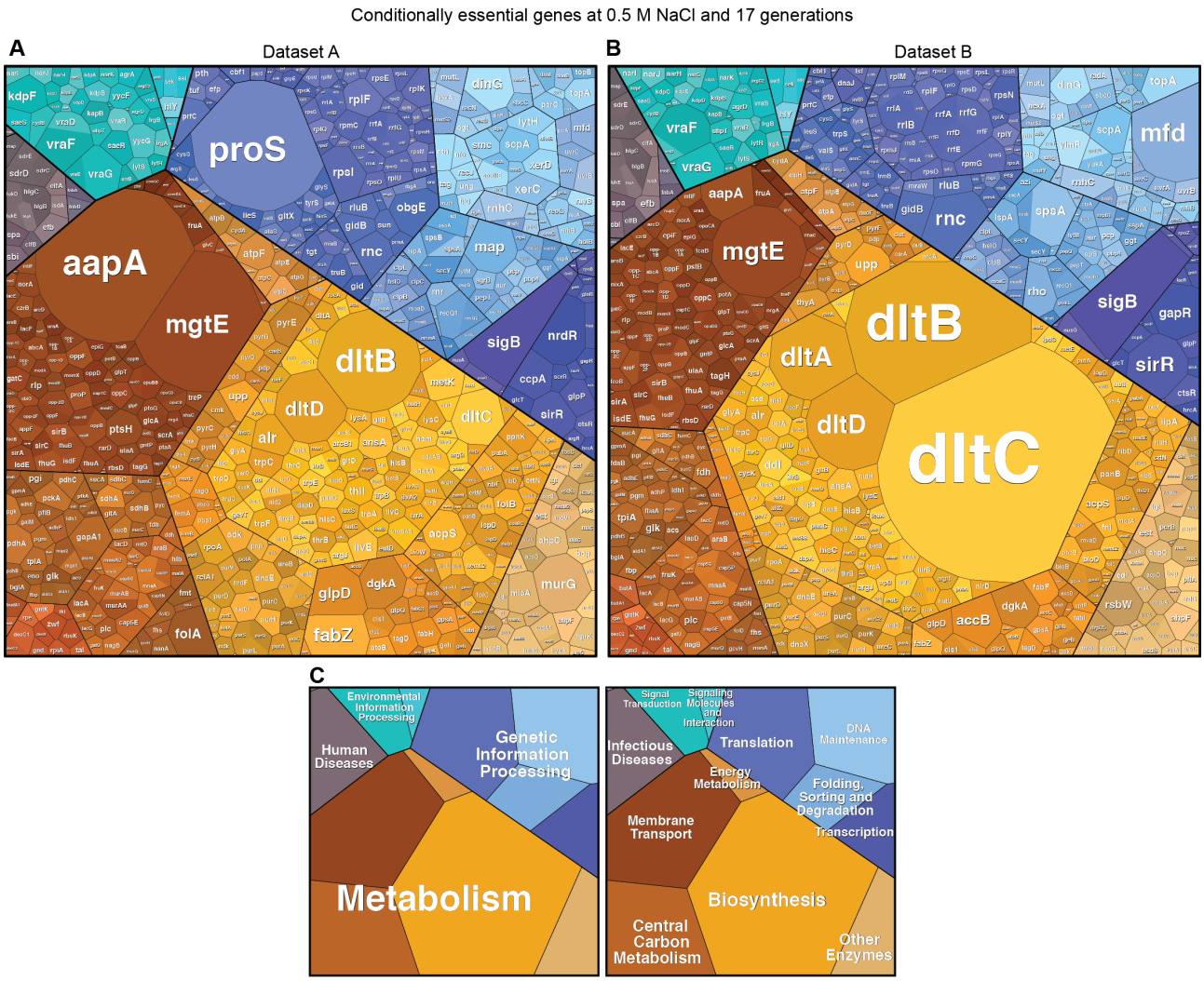

Supplementary Fig. 3. Voronoi diagram-based visualization of *S. aureus* conditionally essential genes when exposed to 0.5 M NaCl.

Conditionally essential *S. aureus* genes from replicate A (A) and replicate B (B) grown in 0.5 M NaCl for 17 generations were mapped to cellular functions with area sizes adjusted to their essentiality regardless of p- or q-value. The larger the area, the lower the number of transposon insertions in stress condition as compared to the LBN control condition. Colors of polygons indicate cellular functions as detailed in (C).

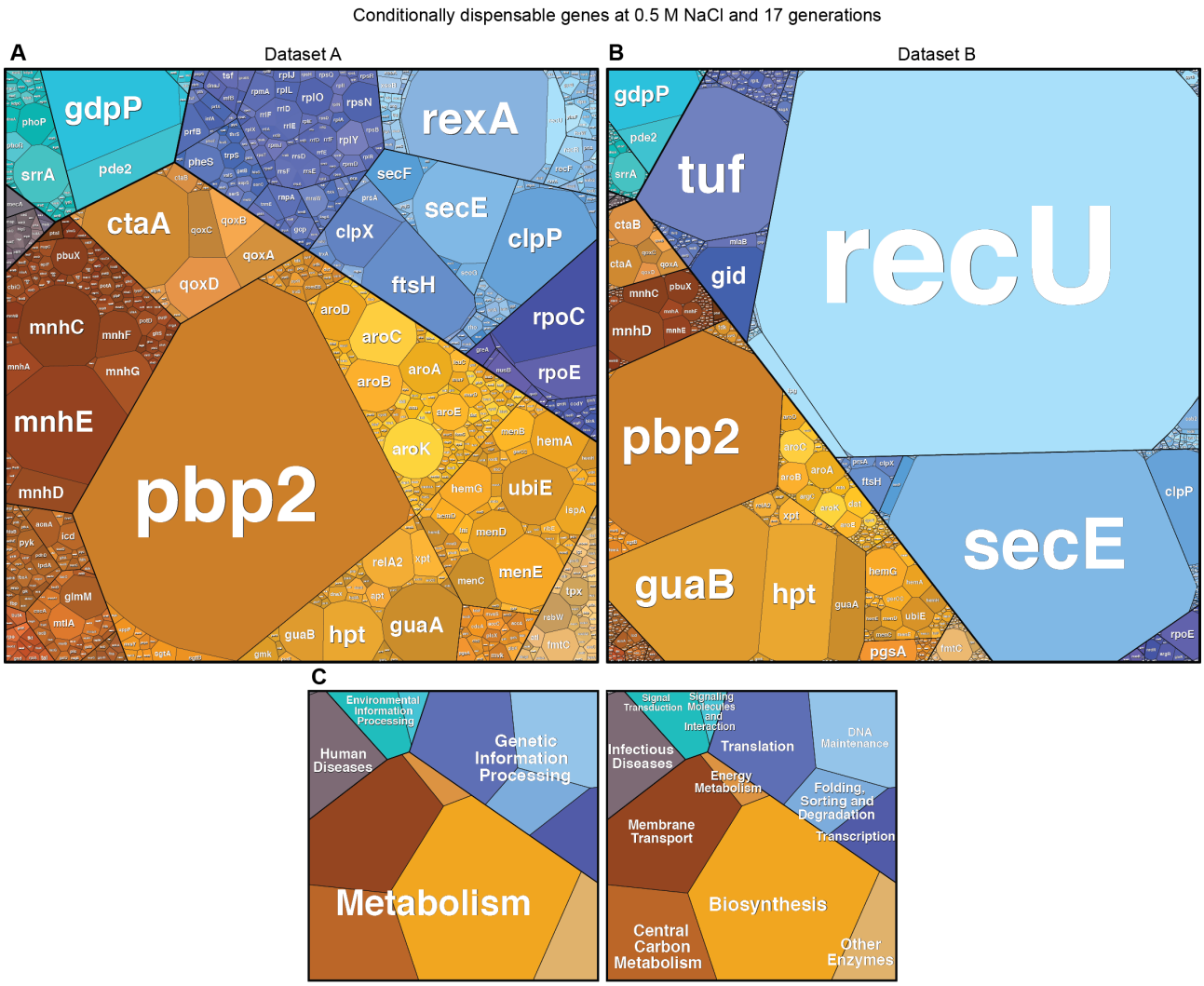

Supplementary Fig. 4. Voronoi diagram-based visualization of *S. aureus* conditionally dispensable genes when exposed to 0.5 M NaCl.

Conditionally dispensable *S. aureus* genes from replicate A (A) and replicate B (B) grown in 0.5 M NaCl for 17 generations were mapped to cellular functions with area sizes adjusted to their dispensability regardless of p- or q-value. The larger the area, the higher the number of transposon insertions in the stress condition as compared to the LBN control. *recU* was scaled to 1/5 of the original ratio to preserve space. Colors of polygons indicate cellular functions as detailed in (C).

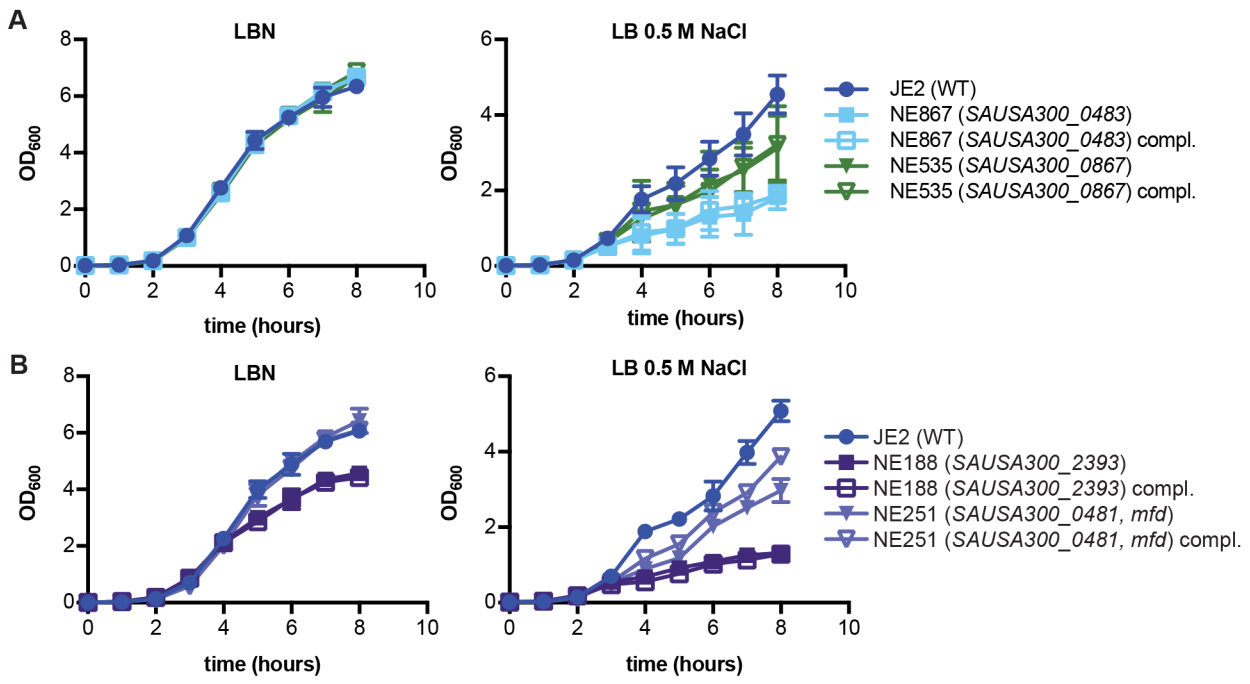

Supplementary Fig. 5. Complementation analysis using *S. aureus* mutants with transposon insertions in putative salt resistance genes.

(A) Growth curves. *S. aureus* strains JE2 (WT), NE867 and NE535 with integrated pCL55 and *S. aureus* strains NE867 and NE535 with respective complementation plasmids were grown in either LBN or LB 0.5 M NaCl and their growth monitored by determining OD_{600} readings.

(B) As in (A) but using strains JE2 piTET (WT) or NE188 and NE251 containing plasmid piTET or the respective complementation plasmid. Strains were grown in LBN or 0.5 M NaCl LB medium supplemented with 100 ng/ml Atet. All experiments were conducted three times and the means and standard deviations were plotted.

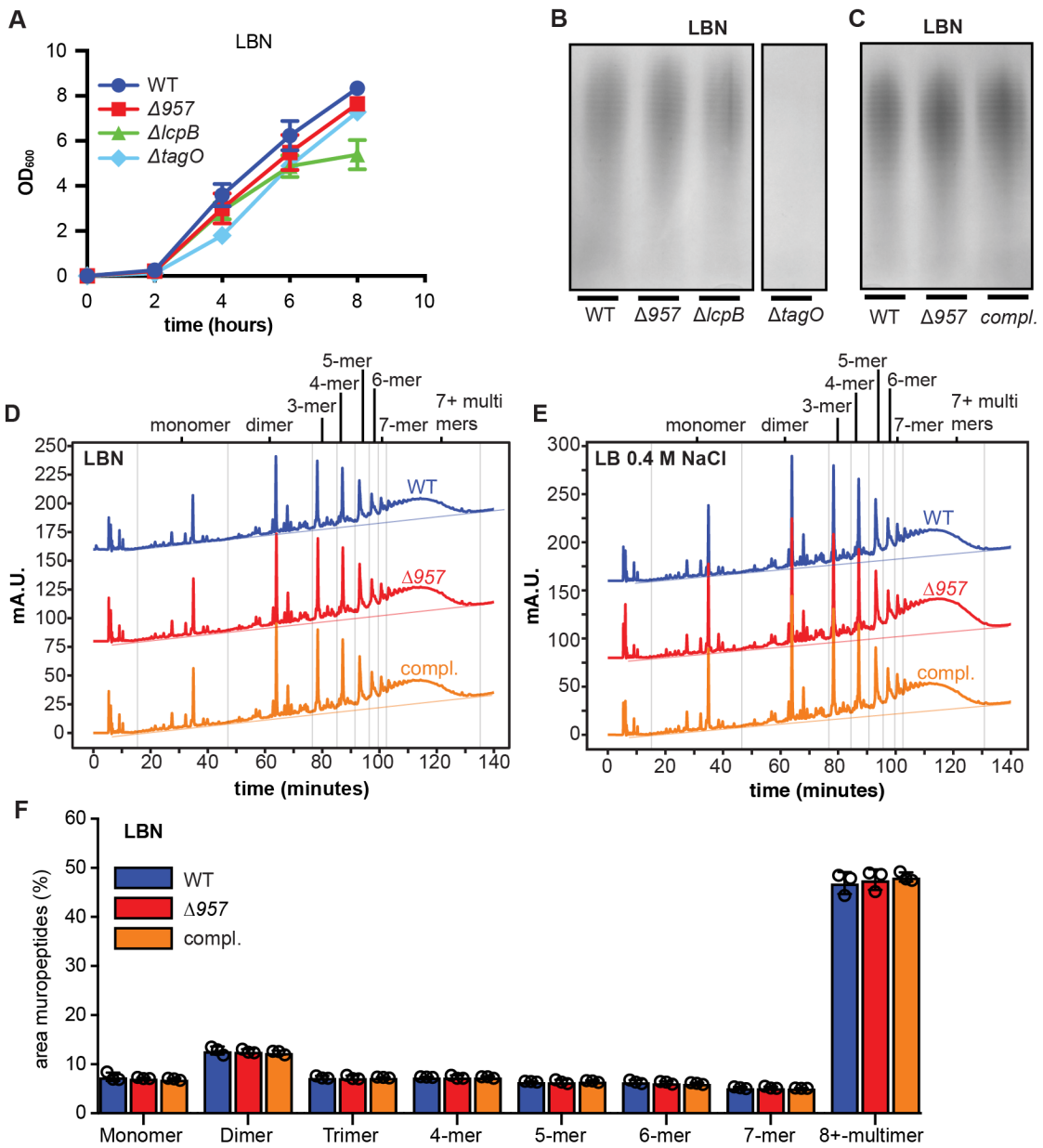

Supplementary Fig. 6. Investigating the involvement of gene *957* in cell wall homeostasis.

(A) Growth curves using strains with mutations in WTA synthesis genes. *S. aureus* strains LAC* (WT), LAC*Δ*957* (Δ*957*), LAC*Δ*lcpB* (Δ*lcpB*) and LAC*Δ*tagO* (Δ*tagO*) were grown in LBN and growth monitored by measuring OD_{600} readings. The experiment was performed three times and means and standard deviations were plotted.

(B) Detection of WTA. WTA was isolated from the strains described in (A) following growth in LBN medium, then subjected to electrophoresis on polyacrylamide gels and visualized by silver staining. One representative result is shown out of three independent experiments.

1185 (C) Detection of WTA. Experimental setup is the same as in (B) but using the strains LAC* piTET (WT),
1186 LAC*Δ*957* piTET (Δ*957*) and LAC* Δ*957* piTET-*957* (compl.).
1187 (D) Muropeptide profile. The same strains as described in panel (C) were grown in LBN medium and
1188 the peptidoglycan isolated, digestion with mutanolysin and the muropeptides subsequently
1189 separated by HPLC. Shown are representative chromatograms from three independent
1190 experiments. Retention time ranges of mono-, di- and higher multi-mers are indicated by vertical
1191 lines.
1192 (E) Muropeptide profiles. As in (D) but bacteria were grown in LB 0.4 M NaCl.
1193 (F) Muropeptide quantification. The areas under the peaks from the chromatograms shown in panel
1194 (D) and two additional replicates were quantified for each mono-, di- or multimer area. Bars
1195 represent mean and error bars standard deviations from three independent experiments. For
1196 statistical analyses, a two-way ANOVA was performed, followed by a Dunnett's post-hoc test but no
1197 significant changes were present between either the wild type and the mutant or the wild type and
1198 the deletion strain. Where induction was necessary, the medium was supplemented with 100 ng/µl
1199 Atet.

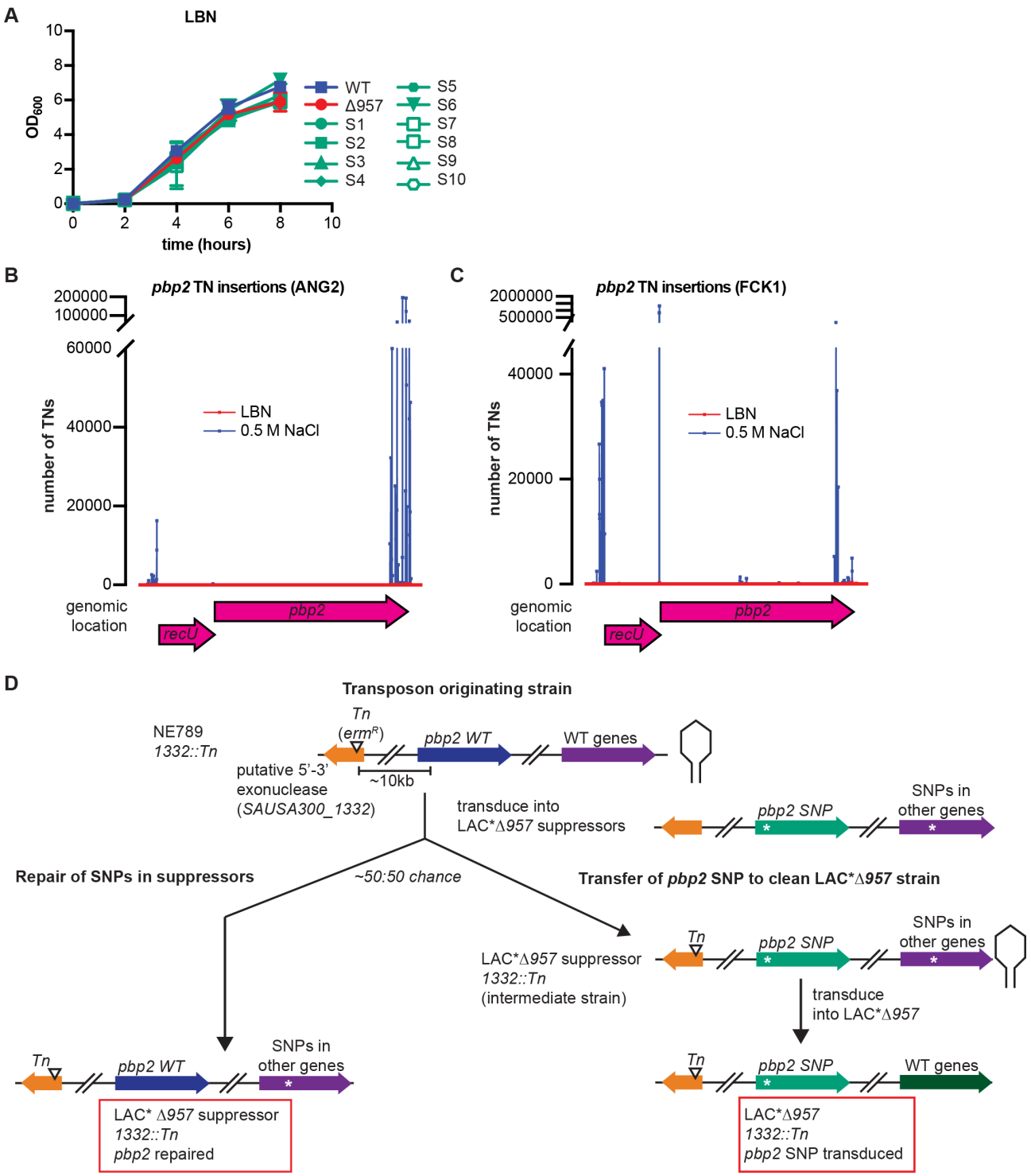

Supplementary Fig. 7. Growth of Δ*957* suppressor strains and schematic of the co-transduction strategy for complementation analysis.

(A) Growth curves of Δ*957* suppressor strains. Strains LAC* (WT), LAC*Δ*957* (Δ*957*) and LAC*Δ*957* suppressors S1 trough S10 (S1-S10) were grown in LBN medium and their growth monitored by

1205 taking OD_{600} readings. The experiment was performed three times and means and standard
1206 deviations were plotted.
1207 (B) TN insertion map. Transposon insertions from replicate A (ANG dataset) were mapped to the
1208 *recU*/*pbp2* operon from a library grown in LBN (red) or LB medium containing 0.5 M NaCl salt (blue).
1209 (C) TN insertion map. As in (B) but using replicate B (FCK dataset).
1210 (D) Schematic of phage co-transduction experiment to either repair the *pbp2* SNP in the suppressor
1211 strains (left branch) or to transduce the *pbp2* suppressor mutations into a clean *957* mutant (right
1212 branch). A phage lysate was prepared using an NTML library strain with a transposon insertion in an
1213 unrelated gene (*SAUSA300_1332*) located approximately 10 kb from the *pbp2* SNPs present in the
1214 suppressor strains. This lysate was used for transductions using different LAC*Δ*957* suppressor
1215 strains as recipient strains. With about 50% frequency, the *pbp2* SNPs were exchanged to the wild
1216 type allele by transducing *SAUSA300_1332*::*Tn* and the WT *pbp2* allele producing strain LAC*Δ*957*
1217 suppressor *1332*::*Tn pbp2* repaired (left branch). In the other cases, the *SAUSA300_1332*::*Tn* region
1218 was transferred to a suppressor strain without replacing the *pbp2* SNP (right branch). A phage lysate
1219 prepared on this intermediate strain (LAC*Δ*957* suppressor *1332*::*Tn*) was then used to transduce
1220 the *pbp2* suppressor SNP into a clean LAC*Δ*957* strain, resulting in the clean suppressor strain
1221 LAC*Δ*957 1332*::Tn *pbp2* SNP transduced.

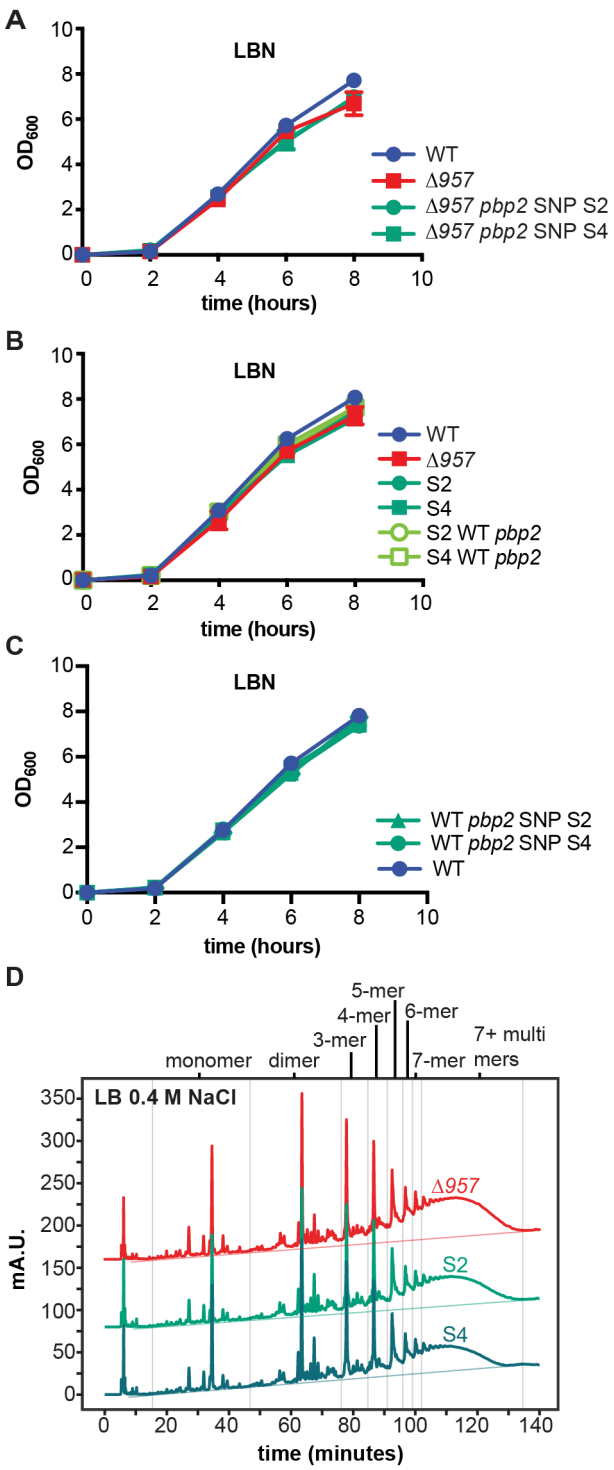

Supplementary Fig. 8. Growth and peptidoglycan analysis of *957* mutant and suppressor strains.

(A) Growth curves using *957* mutants with transduced *pbp2* SNPs. Strains LAC* *1332*::Tn (WT), LAC*Δ*957* *1332*::Tn (Δ*957*), LAC*Δ*957* *1332*::Tn *pbp2* SNP S2 (Δ*957* *pbp2* SNP S2), LAC*Δ*957* suppressor S4 *1332*::Tn (Δ*957* *pbp2* SNP S4) were grown in LBN medium and growth monitored by

1227 determining OD_{600} readings. The means and standard deviations from three independent
1228 experiments were plotted.
1229 (B) Growth curves using *957* suppressor strains carrying a repaired WT *pbp2* gene. Same as in (A)
1230 but using strains LAC* *1332*::Tn (WT), LAC*Δ*957* *1332*::Tn (Δ*957*), LAC*Δ*957* suppressor S2 *1332*::Tn
1231 (S2), LAC*Δ*957* suppressor S4 *1332*::Tn (S4), LAC*Δ*957* suppressor S2 *1332*::Tn repaired WT *pbp2*
1232 (S2 WT *pbp2*), and LAC*Δ*957* suppressor S4 *1332*::Tn repaired WT *pbp2* (S4 WT *pbp2*).
1233 (C) Growth curves using WT strains carrying *pbp2* SNP mutations. Same as in (A) but using strains
1234 LAC* *1332*::Tn (WT), LAC* *1332*::Tn *pbp2* SNP S2 (WT *pbp2* SNP S2) and LAC* *1332*::Tn *pbp2* SNP S4
1235 (WT *pbp2* SNP S4).
1236 (D) Muropeptide profiles. Strains LAC*Δ*957* (Δ*957*), LAC*Δ*957* Suppressor S2 (S2) and S4 LAC*Δ*957*
1237 Suppressor S4 (S4) were grown in LB medium with 0.4 M NaCl, the peptidoglycan was extracted,
1238 digested with mutanolysin, and the muropeptide separated by HPLC. Retention ranges for
1239 monomers, di- and higher oligomers are indicated by vertical lines. The experiment was conducted
1240 with three times and one representative result is shown.
1241